preprint astro-ph/9512122; 1999 ApJ, 510, in press

Creation of ^{7}Li and Destruction of ^{3}He, ^{9}Be, ^{10}B, and ^{11}B in Low Mass Red Giants, Due to Deep Circulation

I.-Juliana Sackmann
W. K. Kellogg Radiation Laboratory 106-38, California Institute of Technology, Pasadena, CA 91125; ijs@krl.caltech.edu

and

Arnold I. Boothroyd[1]
Dept. of Mathematics & Statistics, Monash University, Clayton, VIC 3168, Australia

ABSTRACT

It has been demonstrated that ^{7}Li can be created in low mass red giant stars via the Cameron-Fowler mechanism, due to extra deep mixing and the associated "cool bottom processing". Under certain conditions, this ^{7}Li creation can take the place of the ^{7}Li destruction normally expected. Note that such extra mixing on the red giant branch (RGB) has previously been invoked to explain the observed ^{13}C enhancement. This new ^{7}Li production can account for the recent discovery of surprisingly high lithium abundances in some low mass red giants (a few of which are super-rich lithium stars, with abundances higher than that in the interstellar medium). The amount of ^{7}Li produced can exceed $\log \varepsilon(^7\mathrm{Li}) \sim 4$, but depends critically on the details of the extra mixing mechanism (mixing speeds, geometry, episodicity). If the deep circulation is a relatively long-lived, continuous process, lithium-rich RGB stars should be completely devoid of beryllium and boron. Cool bottom processing leads to ^{3}He destruction in low mass stars; in contrast to the ^{7}Li creation, the extent of ^{3}He depletion is largely independent of the details of the extra mixing mechanism. The overall contribution from solar-metallicity stars (from 1 to 40 $M_\odot$) is expected to be a net destruction of ^{3}He, with an overall ^{3}He survival fraction $g_3 \approx 0.9 \pm 0.2$ (weighted average over all stellar masses); this is in contrast to the conclusion from standard dredge-up theory, which would predict that stars are net producers of ^{3}He (with $g_3^{\mathrm{dr}} \sim 2.4 \pm 0.5$). Population II stars experience even more severe ^{3}He depletion, with $0.3 \lesssim g_3 \lesssim 0.7$. Destruction of ^{3}He in low mass stars is consistent with the requirements of Galactic chemical evolution models; it would also result in some relaxation of the upper bound

[1]Present address: W. K. Kellogg Radiation Laboratory 106-38, California Institute of Technology, Pasadena, CA 91125; aib@krl.caltech.edu

on the primordial (D+^{3}He)/H abundance, thus relaxing the lower bound on the cosmic baryon density Ω_b from Big Bang nucleosynthesis calculations. For reference, we also present the effects of standard first and second dredge-up on the helium, lithium, beryllium, and boron isotopes.

Subject headings: Galaxy: abundances — nuclear reactions, nucleosynthesis, abundances — stars: abundances — stars: AGB and Post-AGB

1. Introduction

For some time, it has been known that stars super-rich in lithium exist, with abundances much higher than they could have been endowed with at birth, i.e, larger than the present interstellar medium value. A much clearer understanding of these super-rich lithium stars was provided by the recent Magellanic Cloud observations of Smith & Lambert (1989, 1990), who obtained for the first time a luminosity range for lithium-rich asymptotic giant branch (AGB) stars. They found that the most luminous AGB stars were lithium-rich, in excellent agreement with the predictions of theoretical models of hot bottom burning (Sackmann, Smith, & Despain 1974; Scalo, Despain, & Ulrich 1975; Sackmann & Boothroyd 1992, 1995, 1999). Hot bottom burning is predicted to occur occur only in the most massive AGB stars (between ~ 4 and $\sim 7\ M_\odot$), which are also the most luminous ones (Iben 1975; Blöcker & Schönberner 1991; Lattanzio 1992; Sackmann & Boothroyd 1992, 1995, 1999; Boothroyd & Sackmann 1992; Boothroyd, Sackmann, & Ahern 1993). However, some lithium-rich stars do not fit into the above scenario.

During most of the evolution of a star, lithium is destroyed, as it burns at relatively low temperatures. During the pre-main sequence phase, there can be significant lithium destruction for stars of masses $\lesssim 1\ M_\odot$ (see, e.g., D'Antona & Mazzitelli 1984; Proffitt & Michaud 1989; VandenBerg & Poll 1989; Michaud & Charbonneau 1991). During the main sequence phase, considerable lithium destruction is observed in low mass stars ($\lesssim 1.2\ M_\odot$), e.g., the lithium abundance is reduced by 2 orders of magnitude for the Sun; this is generally explained by rotation-induced slow mixing, with some diffusion (see, e.g., Schatzman 1977; Baglin, Morel, & Schatzman 1985; Vauclair 1988; Pinsonneault et al. 1989; Michaud & Charbonneau 1991; Proffitt & Michaud 1991; Charbonnel, Vauclair, & Zahn 1992; Chaboyer, Demarque, & Pinsonneault 1995), though part of this effect might possibly be due to early main sequence mass loss (Boothroyd, Sackmann, & Fowler 1991; Swenson & Faulkner 1992; Whitmire et al. 1995; Guzik & Cox 1995). As stars approach the base of the red giant branch (RGB), the surface lithium abundance declines further by 2 orders of magnitude, as the deepening convective envelope reaches into lithium-depleted interior layers. Thus RGB stars, and AGB stars of $\lesssim 4\ M_\odot$, are expected to have surface lithium abundances from 2 to 4 orders of magnitude below the present interstellar medium value of $\log \varepsilon(^7\mathrm{Li}) \sim 3.3$ (where $\log \varepsilon(^7\mathrm{Li}) \equiv \log[n(^7\mathrm{Li})/n(\mathrm{H})] + 12$).

In general, this is observed to be the case; Population I red giants usually have lithium abundances lying in the range $-1 \lesssim \log \varepsilon(^7\mathrm{Li}) \lesssim 1$ (Lambert, Dominy, & Sivertsen 1980; Brown et al. 1989). However, a few (of order 1%) of the red giants have been observed to have lithium abundances excess of the standard predictions (Brown et al. 1989; see also Wallerstein & Sneden 1982; Hanni 1984; Gratton & D'Antona 1989; Pilachowski, Sneden, & Hudek 1990; Pallavicini et al. 1990; Fekel & Marschall 1991; Fekel & Balachandran 1993), occasionally having abundances much higher than the present interstellar medium abundance (da Silva, de la Reza, & Barbuy 1995a, 1995b; de la Reza & da Silva 1995; de la Reza, Drake, & da Silva 1996). Frequently, these lithium-rich red giants have large infrared excesses, interpreted as associated circumstellar dust shells. Recently, de la Reza et al. (1997) discovered 20 new lithium-rich giants (doubling the total number known) by searching for lithium lines in giants with infrared excesses. These lithium-rich giants have not yet reached the AGB, and at least some of them are observed to be low mass stars; thus they cannot have experienced ^{7}Li creation via hot bottom burning. This presents a new puzzle, namely, how to explain such high lithium abundances in pre-AGB stars. A related puzzle is presented by observations of field Population II giants by Pilachowski, Sneden, & Booth (1993); they find extra lithium *depletion* by large factors on the RGB *subsequent* to first dredge-up.

Another problem concerns ^{3}He. It is well known that deuterium (D) and ^{3}He are created in the Big Bang. Stars burn their initial D to ^{3}He while still on the pre-main sequence. Low mass stars create ^{3}He pockets in their interior during main sequence burning, as first pointed out by Iben (1967), which will subsequently be dredged up to the surface on the RGB, and injected into the interstellar medium via stellar mass loss on the RGB and AGB. Recent measurements of ^{3}He mass fractions of ~ 0.001 in the low-mass planetary nebulae NGC 3242 and IC 289 confirm that this does indeed occur in at least some stars (Galli et al. 1997). The sum of D+^{3}He in the interstellar medium was predicted to increase with time, due to this stellar processing. The observed solar ratio (D+^{3}He)/H $\approx 4 \times 10^{-5}$ has thus been used as an upper bound on the primordial ratio, in order to constrain Big Bang nucleosynthesis models (see, e.g., Steigman 1985); it provides the strongest lower limit on the baryon to photon number ratio $\eta \geq 3 \times 10^{-10}$, and thus to the baryon density of the universe $\Omega_b \geq 0.01 h^{-2}$ (where h is the Hubble constant in units of $100\,\mathrm{km\,s^{-1}\,Mpc^{-1}}$).

Rood, Bania, & Wilson (1984) pointed out that the apparent observed trend with Galactocentric radius of the ^{3}He abundances in H II regions was the opposite of what one would expect if the Galactic ^{3}He abundance was increasing with time due to stellar processing. More recent data (Rood et al. 1998; Bania et al. 1997) show no significant trend of the ^{3}He abundance in H II regions as a function of either Galactocentric radius or metallicity, with an average abundance of $^3\mathrm{He/H} = 1.5^{+1.0}_{-0.5} \times 10^{-5}$. Some extragalactic measurements of deuterium have recently appeared; a high ratio D/H $\approx 2 \times 10^{-4}$ recently observed in a high-redshift ($z = 3.32$) absorption system in the quasar Q0014+813 (Songaila et al. 1994; Carswell et al. 1994; Rugers & Hogan 1996a) has sparked new interest in deuterium and ^{3}He, since this observation implied a much larger primordial (D+^{3}He)/H value than had been inferred from the Galactic observations. More recently, Rugers & Hogan (1996b) measured $\mathrm{D/H} = 1.9^{+1.6}_{-0.9} \times 10^{-4}$ in another absorber of Q0014+813 (at redshift

$z = 2.798$). If the observed absorption lines do indeed correspond to deuterium and not some coincidental interloper cloud happening to lie at the corresponding velocity, then this leads to correspondingly lower values of $\eta \lesssim 1.7 \times 10^{-10}$ and $\Omega_b \lesssim 0.006h^{-2}$, close to the baryon density $\Omega_b \approx 0.003$ observed in stars and gas, eliminating the need for the existence of large amounts of baryonic dark matter. These observations also imply a decline by a factor of order 6 from the primordial (D+^{3}He)/H value to the presolar value. Galactic chemical evolution models can obtain such a decline only if low mass stars destroy ^{3}He, instead of creating it; even a *low* primordial D/H value tends to result in excessive amounts of ^{3}He at the present epoch if stars create ^{3}He (see, e.g., Yang et al. 1984; Walker et al. 1991; Steigman & Tosi 1992; Vangioni-Flam, Olive, & Prantzos 1994; Galli et al. 1994, 1995) — note that a low value of D/H = $[2.3 \pm 0.3\ (\text{stat}) \pm 0.3\ (\text{syst})] \times 10^{-5}$ has been measured in an absorber at redshift $z = 3.572$ of the quasar $1937 - 1009$ (Tytler & Fan 1994; Tytler, Fan, & Burles 1996), and that deuterium abundances in quasar absorbers are still being debated (see, e.g., Tytler, Burles, & Kirkman 1996; Rugers & Hogan 1997; Webb et al. 1997). Galli et al. (1994, 1995) suggested that a low-energy resonance in the $^3\text{He} + {}^3\text{He}$ reaction could increase this rate sufficiently for low mass stars to become net destroyers of ^{3}He. Hogan (1995) suggested a less speculative mechanism, namely, the extra deep mixing below the conventional convective envelope on the RGB, which is generally invoked to explain the anomalously low $^{12}\text{C}/^{13}\text{C}$ ratios observed in low mass stars (below the $^{12}\text{C}/^{13}\text{C}$ values resulting from first dredge-up).

Over the last two decades, the need for some such deep mixing process on the RGB has been pointed out by many investigators, in order to understand the puzzle of the low $^{12}\text{C}/^{13}\text{C}$ ratios observed in low mass Population I RGB stars, and the ^{12}C depletion and the [O/Fe] – [Na/Fe] anticorrelation discovered in low mass Population II RGB stars (see, e.g., Dearborn, Eggleton, & Schramm 1976; Genova & Schatzman 1979; Sweigart & Mengel 1979; Gilroy 1989; Gilroy & Brown 1991; Dearborn 1992; Smith & Tout 1992; Charbonnel 1994, 1995, 1996; Boothroyd, Sackmann, & Wasserburg 1995, hereafter BSW95; Wasserburg, Boothroyd, & Sackmann 1995, hereafter WBS95; Denissenkov & Weiss 1996; Charbonnel, Brown, & Wallerstein 1998). Recently, BSW95 and WBS95 suggested that such deep circulation might also occur in AGB stars of low mass, in order to account for the anomalously low ^{18}O abundances observed in these stars.

In this paper, we present consistent computations of the effects of standard first and second dredge-up (in RGB and AGB stars, respectively) on ^{7}Li and ^{3}He. In addition, we have included ^{9}Be, ^{10}B, and ^{11}B in our calculations, since they are also destroyed at relatively low temperatures in stars, and therefore can provide additional signatures of stellar mixing. For completeness, we include the results for ^{4}He. We also present calculations of the effects on these isotopes of " cool bottom processing" (CBP). In this process, deep extra mixing transports envelope material into the outer wing of the hydrogen-burning shell, where it undergoes partial nuclear processing, and then transports the material back out to the envelope. We have modelled CBP by a deep circulation process, determining some of the free parameters of our model by requiring that our computations yield results that agree with the observed RGB $^{12}\text{C}/^{13}\text{C}$ ratios. The CNO isotopes for these models are discussed in detail in Boothroyd & Sackmann (1999).

2. Methods

We considered stars of 29 different masses from 0.85 to 9.0 $M_\odot$, evolving them self-consistently from the pre-main sequence through first dredge-up up to either the helium core flash (which terminates the RGB for low mass stars), or through second dredge-up to the first helium shell flash (for intermediate mass stars and some low mass stars), or to core carbon ignition during second dredge-up (for higher masses). For evolutionary program details, see Boothroyd & Sackmann (1988), Sackmann, Boothroyd, & Fowler (1990), and Sackmann, Boothroyd, & Kraemer (1993).

For solar metallicity, we used a helium mass fraction $Y = 0.28$, with solar CNO abundances. For lower metallicities, we reduced Y (taking $\Delta Y/\Delta Z \approx 2$), and increased the oxygen content, approximating the observed trend by [O/Fe] $\propto -0.5$[Fe/H] for [Fe/H] ≥ -1, and constant [O/Fe] $= +0.5$ for [Fe/H] < -1 (see Timmes, Woosley, & Weaver 1995, and references therein). A fuller discussion of the CNO elements is given in Boothroyd & Sackmann (1999). In addition to solar metallicity ($Z = 0.02$), we considered metallicities appropriate to the Magellanic Clouds ($Z = 0.012$ and 0.007, with [Fe/H] ≈ -0.35 and -0.7, respectively), an intermediate value of $Z = 0.003$ ([Fe/H] ≈ -1.2), a Population II metallicity of $Z = 0.001$ ([Fe/H] ≈ -1.7), and an extreme Population II metallicity of $Z = 0.0001$ ([Fe/H] ≈ -2.7). Since stars convert deuterium to ^{3}He on the pre-main sequence, our program lumps deuterium in with ^{3}He; our initial ^{3}He abundance is actually the sum of deuterium and ^{3}He. Since the variation of (D+^{3}He) as a function of time (or metallicity) is not well known, we generally chose an initial ratio $^3\mathrm{He}/^4\mathrm{He} = 4 \times 10^{-4}$ by number (solar abundances), but also considered extreme values of this ratio, namely, 4×10^{-3} and 4×10^{-5}. For solar metallicity we used a ^{7}Li abundance $\log \varepsilon(^7\mathrm{Li}) = 3.0$, close to that of the present interstellar medium ($\log \varepsilon(^7\mathrm{Li})_{\mathrm{ISM}} \approx 3.3$); for Population II metallicities, we reduced the initial ^{7}Li abundance to $\log \varepsilon(^7\mathrm{Li}) = 2.6$, a factor of 5 below the present cosmic abundance. Note that stellar models which include microscopic diffusion of ^{7}Li suggest that this is a reasonable initial value to match the observations of Spite plateau lithium abundances in Population II stars (Vauclair & Charbonnel 1995), as do models which include rotational effects (Pinsonneault, Deliyannis, & Demarque 1992; Deliyannis, Boesgaard, & King 1995; Vauclair & Charbonnel 1995); it is hard to avoid some main sequence ^{7}Li depletion in these stars. Beryllium and boron isotopes were considered only for the cases $Z = 0.02$ and $Z = 0.001$; we used solar abundances ($\mathrm{Be/H} = 1.3 \times 10^{-11}$, $\mathrm{B/H} = 4 \times 10^{-10}$, and $^{11}\mathrm{B}/^{10}\mathrm{B} = 4.0$, by number: Grevesse 1984), scaled linearly with metallicity. Note that initial abundances of the light elements are generally not critical, as the depletion factors that we report in this paper are insensitive to the absolute starting value.

Mass loss on the RGB and AGB was included via a Reimers' (1975) wind, with mass loss parameter $\eta \approx 0.6$, as discussed in Boothroyd & Sackmann (1999) (see also Sackmann et al. 1993); values up to $\eta = 1.4$ for Population I cases with masses $> 2.5\ M_\odot$ were tested, but the amount of mass lost was still insignificant at the points where first and second dredge-up take place. We used the OPAL 1995 interior opacities (Iglesias & Rogers 1996), and Alexander molecular opacities (Alexander & Ferguson 1994) at low temperatures; these latter require a value of $\alpha = 1.67$ (where α is the ratio of the convective mixing length to the pressure scale height) in order to obtain

a correct model of the Sun (Sackmann et al. 1990, 1993). Tests were made using older opacity tables. Use of the interior opacities from the Los Alamos Opacity Library (LAOL: from J. Keady 1985, private communication) yielded only slightly different amounts of dredge-up (Boothroyd & Sackmann 1999), while use of molecular opacities from Sharp (1992) required a value of $\alpha = 2.1$ but had no effect on dredge-up. (Note that the value of α has almost no effect on the depth of dredge-up, as has already been noted by Charbonnel 1994). Nuclear reaction rates from Caughlan & Fowler (1988) were used, except for the ^{17}O-destruction reactions $^{17}\mathrm{O}(p,\alpha)^{14}\mathrm{N}$ and $^{17}\mathrm{O}(p,\gamma)^{18}\mathrm{F}(e^{+}\nu)^{18}\mathrm{O}$, where the rates of J. C. Blackmon (1996, private communication; from measurements of Blackmon et al. 1995) or of Landré et al. (1990) were used.

For cool bottom processing (CBP), parametric computations were performed, with envelope structures obtained from full evolution models of a 1 $M_{\odot}$ star in the appropriate stages of evolution. Two types of models were considered. In the first type, as described in WBS95, the star's structure was taken to be unchanging in time ("single episode"); it was taken at the point on the RGB where CBP is expected to begin (when the hydrogen shell erases the composition discontinuity left behind by first dredge-up). The CBP was then computed over time period less than or comparable to the RGB lifetime. In the second type of model, the change in envelope structure as the star climbs the RGB was taken into account by interpolating between full evolution models at 15 points on the RGB ("evolving RGB"). The CBP was assumed to start when the hydrogen shell erases the composition discontinuity from first dredge-up, and continue until the tip of the RGB was reached. For these "evolving RGB" cases, metallicities $Z = 0.02$, 0.007, 0.001, and 0.0001 were considered (taking structures from the relevant full evolution models), and higher masses were simulated by adding envelope mass, and starting at the appropriate (higher-luminosity) RGB position (this should be a good approximation, since the structure near the burning shell on the RGB is almost independent of the envelope mass). Isotopic abundances were taken from full evolutionary models, except for ^{7}Li, where an additional main sequence depletion by a factor of 50 was assumed for the 1 $M_{\odot}$ case (note that the observed main sequence ^{7}Li depletion in low mass stars cannot be predicted by standard stellar models).

In our two-stream "conveyor-belt" circulation model for CBP, matter from the bottom of envelope convection streamed downward, reaching a maximum temperature T_P, then returned upward and was mixed with the convective envelope (i.e., a composition advection equation with nuclear burning, and no mixing between downward and upward streams). Envelope and stream compositions were followed through time. We assumed that the temperature difference $\Delta \log T = \log T_P - \log T_H$ between the bottom of mixing and the bottom of the hydrogen-burning shell was constant, and treated it as a free parameter; values selected for discussion were those satisfying the observational data, as discussed in WBS95 and Boothroyd & Sackmann (1999). For a thin H-burning shell, assuming constant $\Delta \log T$ is roughly equivalent to assuming extra mixing always reaches down to the same value of the molecular weight gradient $\nabla\mu$.

For CBP in the "single episode" circulation models, $\Delta \log T \approx 0.17$ yielded a reasonable match to the observed $^{12}\mathrm{C}/^{13}\mathrm{C}$ ratio on the RGB ($\sim 13 \pm 3$ for a 1.2 $M_{\odot}$ star, or ~ 11 for a 1.0 $M_{\odot}$ star:

see Gilroy 1989), after a processing time $t_{\rm mix:RGB} \approx 1.25 \times 10^7$ yr (see Fig. 7). During this time, the star's luminosity increases by only 60% (Sackmann et al. 1993), so the assumption of static envelope structure is not unreasonable (the luminosity increase is by a factor of 100 at the tip of the RGB, after a time $\tau_{\rm RGB} \sim 7 \times 10^7$ yr). For CBP in the "evolving RGB" circulation models, $\Delta \log T = 0.262 \pm 0.010$ matched the above observed carbon isotope ratios on the RGB (Fig. 9a; see also Boothroyd & Sackmann 1999).

The other key free parameter was the stream mass flow rate $\dot{M}_p$. This must be slower than that of convection in RGB or AGB envelopes ($\dot{M}_p \ll \dot{M}_{\rm conv} \sim 1\ M_\odot$/yr), while the streams must move faster than the speed with which the H-shell burns its way outward ($\dot{M}_p \gtrsim \dot{M}_c$). We explored a wide range of $\dot{M}_p$ values. For equal downward and upward velocities, the fractional areas at the base of the convective envelope occupied by downward and upward streams are equal. The downward stream then spends a time $\Delta t_d = 0.5\,\Delta M_r/\dot{M}_p$ in a layer ΔM_r, the upward stream spending the same time Δt_u there on its way out. When downward and upward velocities (and respective fractional areas f_d and f_u) are *not* equal, these times become $\Delta t_d = f_d \Delta M_r/\dot{M}_p$ and $\Delta t_u = f_u \Delta M_r/\dot{M}_p$. The total time spent in any mass layer is independent of f_d and f_u, for $f_d + f_u = 1$; thus the total amount of nuclear burning is generally independent of f_u/f_d. The ^{7}Li production via the Cameron-Fowler mechanism (Cameron 1955; Cameron & Fowler 1971) is an exception; it *does* depend on f_u, which affects the speed with which ^{7}Be is transported upwards, and thus the amount which survives to reach cool layers before decaying into ^{7}Li. Let $f \equiv f_u/f_d$; besides $f = 1$ (i.e., $f_d = f_u = 0.5$), we considered $f = 9$ and 99.

3. Results

We present first and second dredge-up results from standard stellar models, and cool bottom processing (CBP) results from our "single episode" and "evolving RGB" circulation models of extra mixing. Note that some results for ^{4}He, ^{3}He, and the CNO isotopes are tabulated in Boothroyd & Sackmann (1999); more detailed tables are available from the authors[2].

3.1. Standard First and Second Dredge-up

Figure 1a presents the mass layer M_r/M down to which the convective envelope reaches, at its deepest penetration during standard first and second dredge-up (for stars of $> 7\ M_\odot$, the depth of second dredge-up is shown at the moment when the program failed during core carbon ignition). Note that we define "second dredge-up" in low mass stars as the stage of deepest convective penetration on the early AGB, even if this is shallower than first dredge-up. Figure 1b displays the

[2] Tables may be obtained by contacting A. Boothroyd at aib@krl.caltech.edu or from A. Boothroyd's Web page at http://www.krl.caltech.edu/~aib/

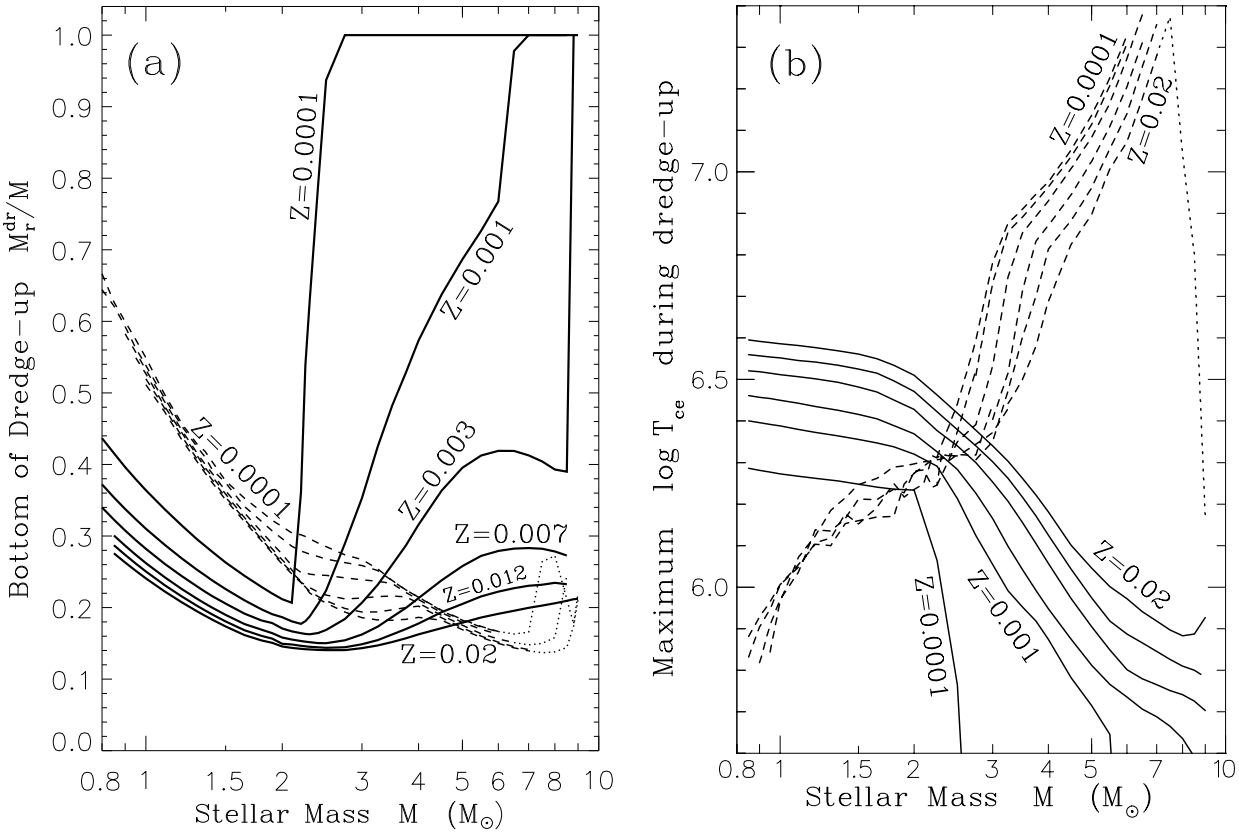

Fig. 1.— (a) Maximum depth in mass of the convective envelope ($M_r^{\rm dr}$), relative to the initial stellar mass M, of first and second dredge-up (*solid* and *dashed curves*, respectively) as a function of stellar mass M. The metallicities are indicated on the curves for first dredge-up; the second dredge-up curves are in the same order. For $Z = 0.02$, 0.007, and 0.0001, the *dotted* continuations of the dashed curves show the depth reached by second dredge-up at the point where the program failed during core carbon ignition. (b) The maximum temperature $T_{\rm ce}$ at the bottom of the convective envelope during first and second dredge-up (*solid* and *dashed curves*, respectively) for the same metallicities as (a); for $Z = 0.02$, the value of $T_{\rm ce}$ is also shown at the time of core carbon ignition, for stars of mass $> 7\,M_\odot$ (*dotted* continuation of dashed curve).

corresponding temperatures $T_{\rm ce}$ at the base of the convective envelope. For $Z = 0.02$ stars of mass $\leq 1\,M_\odot$, there is some burning of ^{7}Li during first dredge-up, when $T_{\rm ce}$ reaches nearly 4×10^6 K. Higher temperatures are attained during second dredge-up in intermediate mass stars, but no ^{7}Li burning takes place in any but the highest mass stars ($\sim 6 - 7\,M_\odot$), as the timescales are too short.

Figure 2 illustrates where in a star's envelope ^{7}Li, ^{9}Be, ^{10}B, and ^{11}B are destroyed, and where in the interior the pocket of ^{3}He has been created, prior to first dredge-up. One sees that ^{7}Li is burned up first, followed by ^{9}Be; further in, ^{11}B and ^{10}B burn at similar depths (^{11}B slightly before ^{10}B). The pocket of ^{3}He peaks considerably deeper in the interior. First dredge-up will

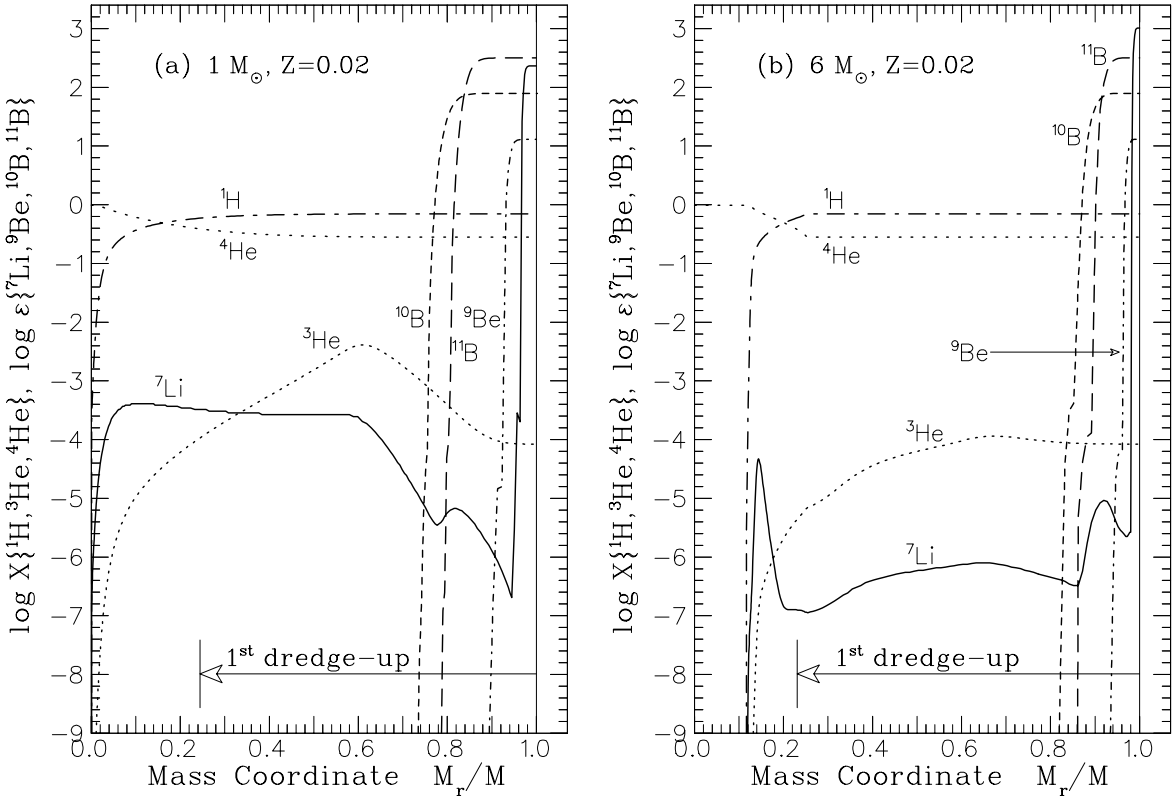

Fig. 2.— The abundance profiles of the light elements as a function of the mass coordinate M_r/M at the end of the main sequence for $Z = 0.02$ stars (a) of 1 $M_\odot$, and (b) of 6 $M_\odot$. The depth of standard first dredge-up on the RGB is shown by the arrows.

dilute the pockets of ^{7}Li, ^{9}Be, ^{11}B, and ^{10}B, and will enrich the surface with ^{3}He from the pocket below. Table 1 illustrates the depths of these pockets in stars of different masses and metallicities, prior both to first dredge-up on the RGB and to second dredge-up on the AGB.

Figure 3 displays the envelope ^{4}He enrichment produced by first and second dredge-up. There is little metallicity dependence; first dredge-up in low mass stars increases the helium mass fraction by $\Delta Y \sim 0.02$, while second dredge-up in $\sim 7\,M_\odot$ stars yields $\Delta Y \sim 0.1$. One can compute the contribution of these stars to the ^{4}He enrichment of the interstellar medium (similar estimates for CNO isotopes are discussed in more detail in Boothroyd & Sackmann 1999). Using the initial–final mass relationship (Weidemann & Koester 1983; Weidemann 1984), one can estimate the envelope mass ejected for a given initial stellar mass. Multiplying mass ejected by the mass fraction of ^{4}He from Figure 3, and weighting the results by an initial mass function $\phi(M) \propto M^{-2.3}$ (Salpeter 1955), one can estimate the contribution to the interstellar medium. Comparing with similar ^{4}He computations for supernovae (Weaver & Woosley 1993), one finds that low and intermediate mass stars ($1 - 12\,M_\odot$) inject nearly as much ^{4}He into the interstellar medium as do supernovae.

Figure 4 is a key diagram. It illustrates the conventional viewpoint that low mass stars ($M \lesssim 4\,M_\odot$) should be a considerable source of ^{3}He in the universe, according to the predictions of standard dredge-up theory. Note that the first and second dredge-up results of Figure 4 are in good agreement ($\sim 10\%$) with the low mass star results of Charbonnel (1995, 1996), the low and intermediate mass star results of Dearborn, Steigman, & Tosi (1996), and the intermediate mass star results of Weiss, Wagenhuber, & Denissenkov (1996) (though the latter find $\sim 30\%$ less ^{3}He dredge-up than the other authors, for stellar masses below 1.5 $M_\odot$). Figure 4 also illustrates the ^{3}He depletion that is expected due to extra mixing in low mass stars, as computed via our "evolving RGB" CBP models (*diamonds* on *long-dashed curves*). For low enough stellar masses, overall depletion of ^{3}He is obtained, relative to its initial abundance. On average, one finds that stars, particularly low-metallicity stars, are net destroyers of ^{3}He in the universe; this is discussed below in § 3.2. (Note that Fig. 4 does *not* show the effect of hot bottom burning in intermediate mass AGB stars, which would destroy almost all the ^{3}He in Population I stars of $4 - 7\,M_\odot$, and in Population II stars of $3.5 - 6\,M_\odot$; Boothroyd & Sackmann 1992; Sackmann & Boothroyd 1999.)

Figure 5 summarizes the reduction of the surface ^{7}Li abundance due to pre-main sequence burning and first and second dredge-up. Pre-main sequence burning (*dot-dashed curve* in Fig. 5) is important only for masses $\lesssim 1.2\,M_\odot$ at near-solar metallicity; there is no significant pre-main sequence ^{7}Li burning in Population II stars of $\geq 0.85\,M_\odot$. Possible effects of main-sequence ^{7}Li

Table 1: Size of the Pockets of ^{7}Li, ^{9}Be, ^{10}B, and ^{11}B Prior to First and Second Dredge-Up [a]

Z, stage	M ($M_\odot$)	$(M - M_r)/M$ dr [b]	^{7}Li	^{9}Be	^{10}B	^{11}B	^{3}He	^{3}He$_p$ [c]	$\frac{^3\mathrm{He}_p}{^3\mathrm{He}_s}$ [d]
0.02,	1.0	0.756	0.037	0.060	0.194	0.152	0.826	0.391	49.
RGB	2.5	0.858	0.0148	0.0312	0.1172	0.0872	0.777	0.369	5.8
	6.0	0.769	0.0132	0.0275	0.1055	0.0770	0.604	0.327	1.37
0.001,	1.0	0.689	0.024	0.055	0.176	0.139	0.724	0.336	54.
RGB	2.5	0.746	0.0104	0.0240	0.0932	0.0696	0.751	0.283	8.0
	6.0	0.0008	0.0080	0.0205	0.0788	0.0575	0.510	0.260	1.69
0.02,	2.5	0.788	0.669	0.717	0.760	0.753	0.783	0.778	1.10
AGB	6.0	0.845	0.559	0.647	0.708	0.691	0.754	0.741	1.01
0.001,	2.5	0.729	0.255	0.324	0.508	0.464	0.659	0.627	1.08
AGB	6.0	0.837	0.0079	0.0204	0.0787	0.0574	0.512	0.260	1.68

[a] Bottom of pocket is defined as point where abundance drops by a factor of 2.

[b] Fraction of the star's mass contained in the convective envelope at the time of deepest dredge-up.

[c] Depth of the ^{3}He peak.

[d] Peak ^{3}He abundance, relative to its surface abundance. Note that the peak subsequently grows somewhat higher than the values quoted here, before it is actually dredged up.

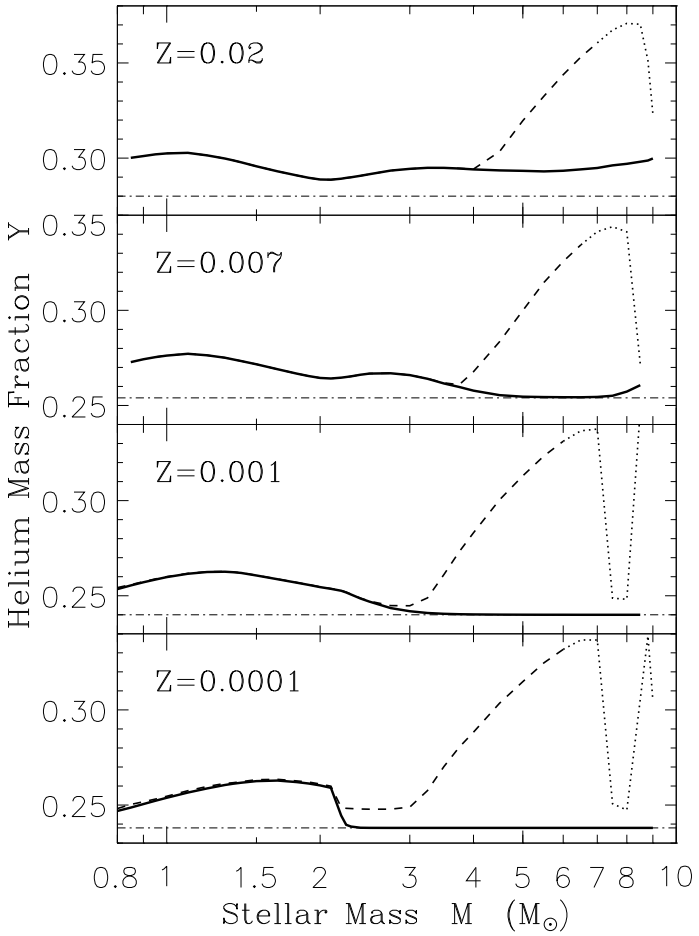

Fig. 3.— Envelope ^{4}He mass fraction Y due to standard first and second dredge-up (*solid* and *dashed curves*, respectively), or at core carbon ignition during second dredge-up (*dotted* continuation of *dashed curves*), as a function of initial stellar mass M for various input metallicities Z. The initial stellar abundance is given by the *dot-dashed lines*.

depletion on the first dredge-up depletion factors of Figure 5 are discussed below.

The ^{7}Li depletion due to first and second dredge-up is usually due entirely to dilution (by a factor of ~ 60) of the surface lithium pocket, and this dilution is relatively insensitive to the stellar mass and metallicity (varying by less than a factor of 3). In addition to dilution, however, there are some cases where ^{7}Li also burns during dredge-up, at the bottom of the (standard) deep convective envelope. This occurs during first dredge-up only for Population I stars of masses $\leq 1\ M_\odot$, and during second dredge-up only for Population I stars of $\sim 7\ M_\odot$ and Population II stars of $\sim 6\ M_\odot$.

Extra mixing on the main sequence can destroy lithium there; one may question whether this would affect the first dredge-up dilution factors. Low mass stars are observed to experience considerable ^{7}Li depletion on the main sequence (see, e.g., Hobbs & Pilachowski 1988, and references therein). This will affect the RGB abundances, but not the dilution factor (since the *size* of the

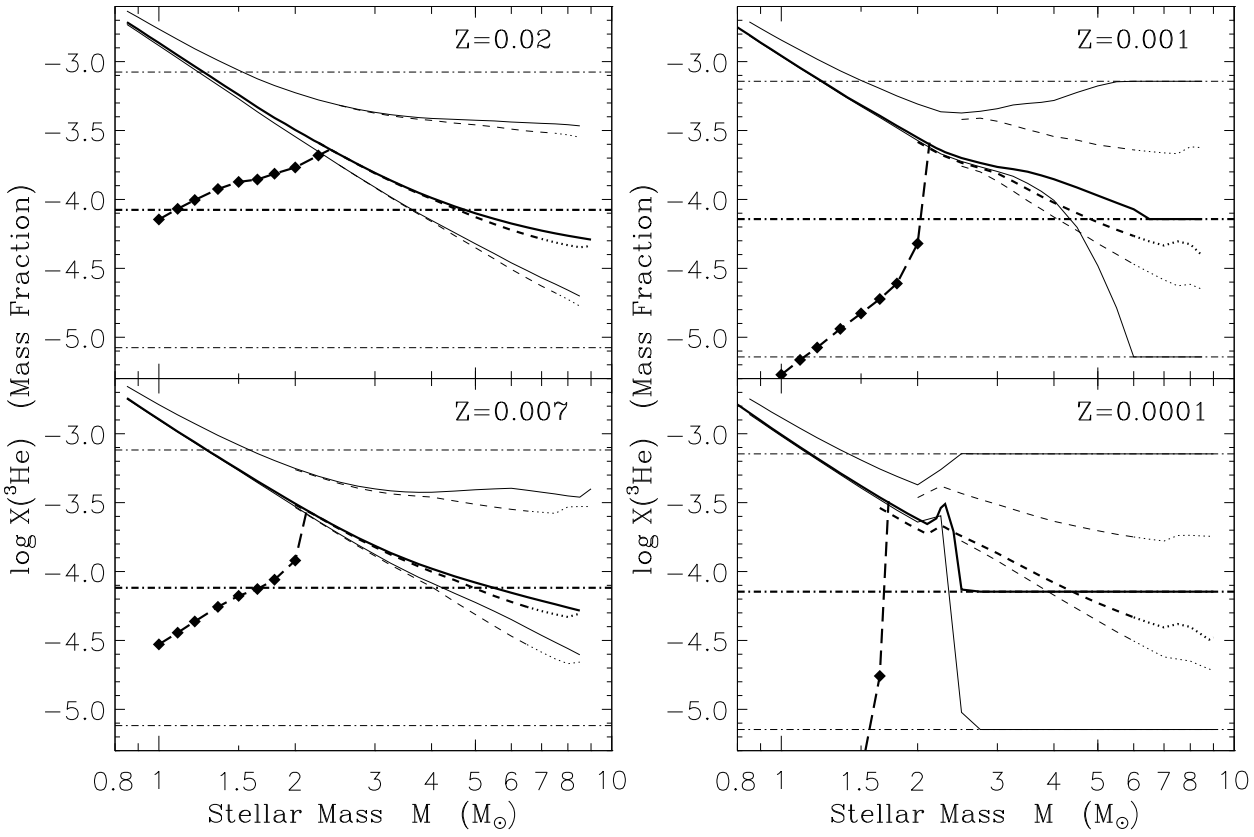

Fig. 4.— Envelope ^{3}He abundance due to standard first and second dredge-up (*solid* and *dashed curves*, respectively), or at core carbon ignition (*dotted* continuation of dashed curves); *dot-dashed lines* show initial stellar ^{3}He abundances. Heavy (central) curves are for our standard initial ratio $^3\mathrm{He}/^4\mathrm{He} = 4 \times 10^{-4}$ by number; light curves are for extreme cases 4×10^{-3} and 4×10^{-5}. *Diamonds* connected by *long-dashed curves* show the effect of cool bottom processing (CBP) on the RGB, from our "evolving RGB" CBP models.

lithium pocket on the main sequence cannot be reduced significantly — it does not extend much below the main sequence convective envelope, at least for stars $\lesssim 1\,M_\odot$). Stars of mass $\gtrsim 1.4\,M_\odot$ do not exhibit reduced *surface* lithium abundances while on the main sequence (see, e.g., Boesgaard & Tripicco 1987; Balachandran 1991). However, there may be some evidence that extra mixing can cause additional lithium depletion in the *interior*, reducing the size of the lithium pocket (and thus increasing the first dredge-up dilution factor). For the Hyades, there is no such evidence: the lithium abundances on the RGB are completely explainable by first dredge-up dilution alone, as pointed out by Duncan et al. (1998). Possible evidence for additional lithium depletion comes from Gilroy's (1989) observations of ^{7}Li in open cluster giants of intermediate mass; non-LTE corrections to the observed lithium abundances (Carlsson et al. 1994) may reduce the effect, but probably will not eliminate it.

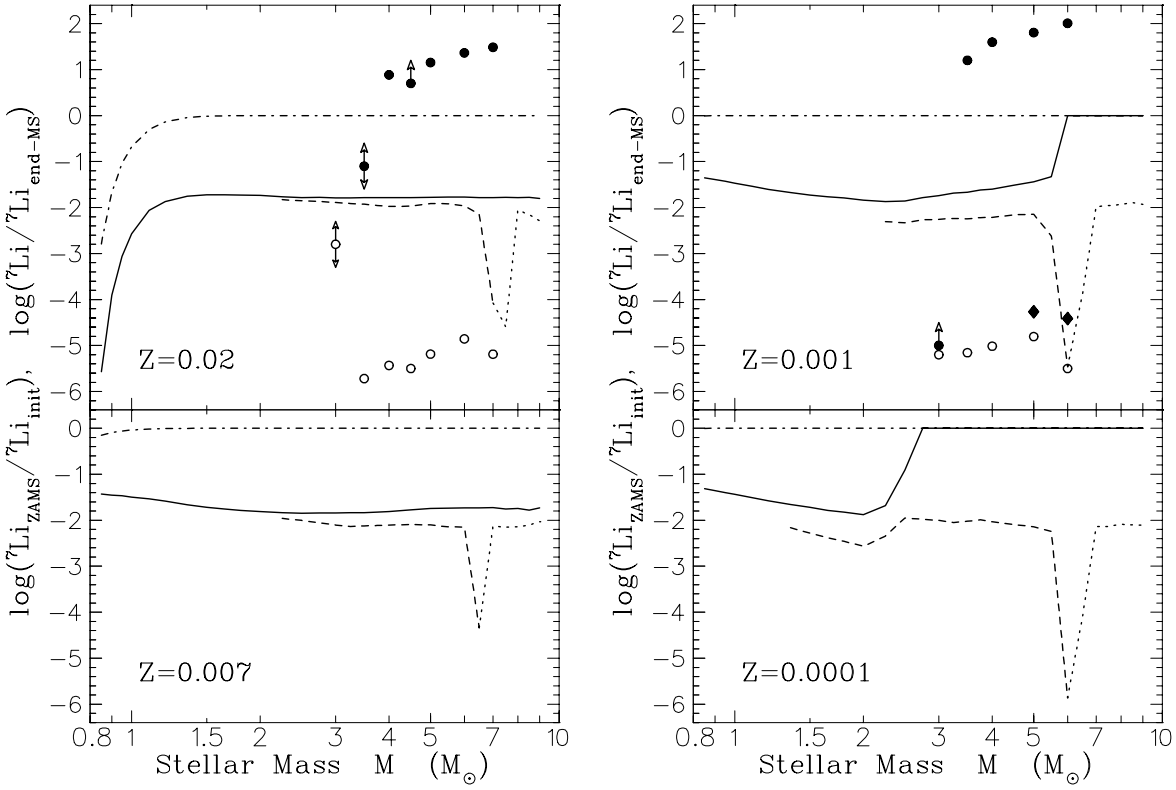

Fig. 5.— Envelope ^{7}Li abundance changes due to standard first and second dredge-up (*solid* and *dashed curves*, respectively), or at core carbon ignition (*dotted* continuation of dashed curves), relative to the values at the end of the main sequence (depletion during the main sequence is not shown). *Dot-dashed curves* show the pre-main sequence ^{7}Li burning, relative to the initial (interstellar medium) value. Separated symbols show the effect of AGB hot bottom burning for $Z = 0.02$ and 0.001: the minimum AGB ^{7}Li abundance at the start of hot bottom burning (*open circles*), peak AGB ^{7}Li abundance (*solid circles*), and final equilibrium hot bottom burning ^{7}Li abundances (*solid diamonds* — note that this equilibrium may not be reached by Population I stars and lower mass Population II stars). Arrows indicate directions of possible shifts in values, as expected from variations in AGB mass loss rates, or from continuation of an incomplete model run (see Sackmann & Boothroyd 1995, 1999).

Figure 5 also summarizes the ^{7}Li creation in AGB stars of $\sim 4 - 7\ M_\odot$ due to hot bottom burning (Sackmann & Boothroyd 1992, 1995, 1999). First, ^{7}Li is burned, being depleted by several orders of magnitude. As hot bottom burning becomes stronger, the Cameron-Fowler mechanism (Cameron 1955; Cameron & Fowler 1971) yields a large increase in the envelope ^{7}Li abundance. Independent of past ^{7}Li history, such super-rich lithium stars attain peak ^{7}Li abundances $10 - 20$ times the present interstellar ^{7}Li abundance, and may contribute significant amounts of ^{7}Li to the interstellar medium (Sackmann & Boothroyd 1995, 1999). The envelope ^{7}Li is produced from ^{3}He; as ^{3}He is burned, the ^{7}Li abundance declines again. If hot bottom burning continues long enough,

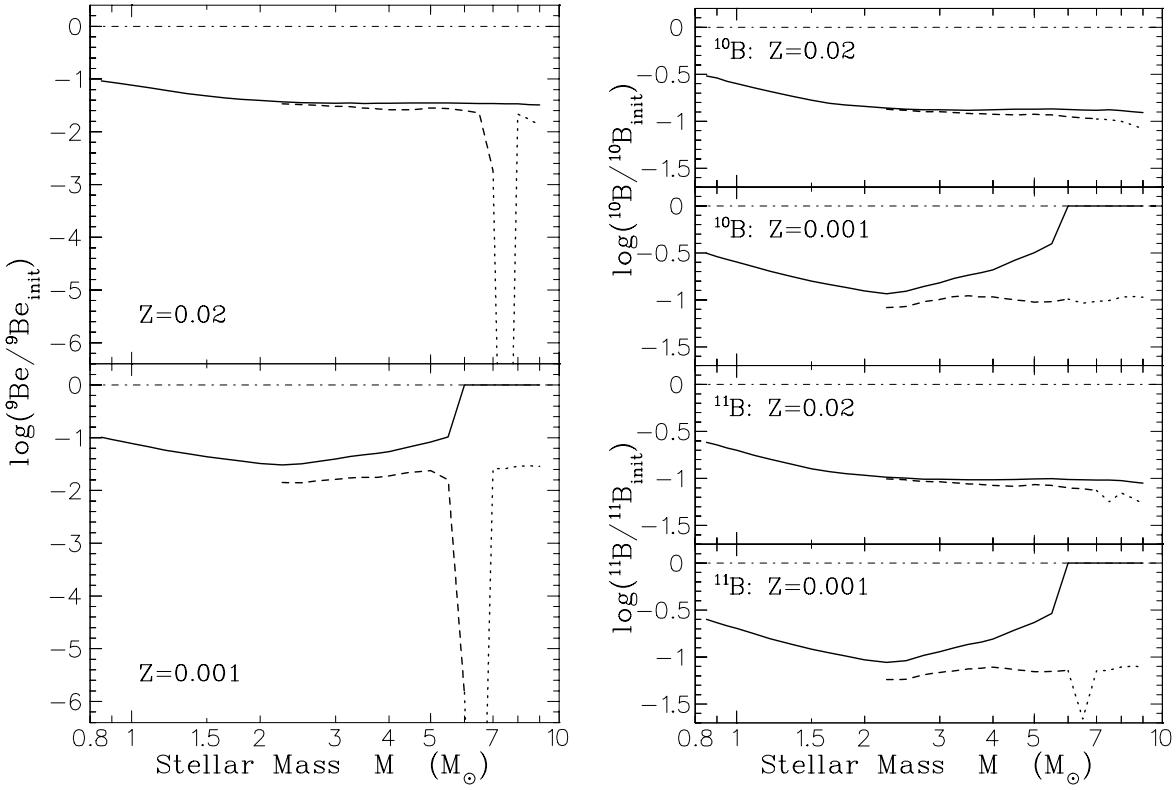

Fig. 6.— Envelope ^{9}Be, ^{10}B, and ^{11}B depletions due to standard first and second dredge-up, as a function of initial stellar mass M, for solar ($Z = 0.02$) and Population II ($Z = 0.001$) metallicities.

^{3}He destruction reaches equilibrium with its creation via the p-p chain, and the ^{7}Li abundance reaches a final value $4 - 5$ orders of magnitude below the interstellar abundance (see 5 and 6 $M_\odot$ $Z = 0.001$ cases in Fig. 5); stellar runs for Population I stars were terminated before this stage was reached, since they approach this final equilibrium much more slowly than Population II stars (and may in fact never reach it at all, depending on the point of onset of the AGB "superwind").

Figure 6 shows the effect of first and second dredge-up on the surface abundances of ^{9}Be, ^{10}B, and ^{11}B, for both solar and Population II compositions. For first dredge-up, the abundance changes are entirely due to dilution; since the extent of the pockets being diluted is greater than for ^{7}Li, the dilution is less. For solar metallicity, this dilution is a factor of ~ 30 for ^{9}Be, and a factor of ~ 10 for ^{10}B and ^{11}B; this dilution is fairly independent of stellar mass except for $M < 2\,M_\odot$ (as was the case for ^{7}Li). The effect of second dredge-up is minor compared to that of first dredge-up; there is burning of ^{9}Be during second dredge-up by as much as several orders of magnitude in stars of $\sim 7\,M_\odot$, but relatively little burning of ^{11}B, and no significant burning of ^{10}B.

There is very little data published on beryllium and boron observations in evolved stars of low or intermediate mass. Boesgaard, Heacox, & Conti (1977) searched for beryllium in four giants in the Hyades cluster, and were only able to obtain upper limits, namely, Be/H $\leq 3.1 \times 10^{-13}$.

For eight Hyades dwarfs, they measured Be/H $\approx 1.0 \times 10^{-11}$ (Boesgaard et al. 1977; Boesgaard & Budge 1989). This implies that the giants had a beryllium dilution factor of ≥ 32. From Gilroy (1989), the turn-off mass of the Hyades is about 2.2 $M_{\odot}$; for this mass, our work shows that standard first dredge-up would give a dilution factor of about 28, which is consistent. Note that possible non-LTE effects were not considered in the above observations.

Note that boron abundances on the RGB should be at least a factor of ~ 30 higher than beryllium abundances there, due to its higher initial abundance. If there were no reduction of the main sequence pockets from extra mixing, there would be an additional factor of 3 from the fact that the boron pocket is three times as big (in mass extent) as the beryllium pocket (see Table 1 or Fig. 2, or the first dredge-up dilution factors from Fig. 6). On the other hand, it is more difficult to observe boron: the 2498 Å line can only be observed from space, and in addition red giant stars have very little flux in the UV (compare to beryllium, where the 3130 Å line can be observed using ground-based telescopes, and there is somewhat more flux). Recently, Duncan et al. (1994, 1998) made the first observations of boron abundances in two red giants in the Hyades. They find [B/H] $= -1.1 \pm 0.2$ in the giants, as opposed to [B/H] $= -0.1 \pm 0.2$ on the main sequence, yielding a boron depletion of order 10, consistent with first dredge-up predictions. They point out that corrections for non-LTE effects for boron in giants are yet to be calculated.

3.2. Deep Circulation on the RGB and AGB

Observations indicate that surface ^{13}C abundances continue to change on the RGB *after* the end of conventional first dredge-up (Gilroy & Brown 1991; Charbonnel 1994; Charbonnel et al. 1998), suggestive of nuclear processing resulting from extra mixing below the base of the convective envelope, i.e., cool bottom processing (CBP). Slow deep circulation tends to be opposed by a gradient in the mean molecular weight μ. A large μ-discontinuity is left behind by first dredge-up. For Population I stars, the post-dredge-up decrease in ^{12}C/^{13}C is observed to commence on the RGB only after the point where the hydrogen shell has subsequently burned its way out to (and destroyed) this "μ-barrier" (see, e.g., Charbonnel 1994; Charbonnel et al. 1998). As discussed in Boothroyd & Sackmann (1999), the ^{12}C/^{13}C observations suggest that CBP begins when the "μ-barrier" is erased, and then "tails off" in a manner intermediate between the behavior assumed in our "single episode" and "evolving RGB" CBP models. Unfortunately, the data are sufficiently sparse that this scenario is not completely certain — for example, an earlier starting point for CBP cannot be *completely* ruled out, though it seems unlikely. Note that the depth of extra mixing in our CBP models was normalized to reproduce the observed ratio ^{12}C/^{13}C ~ 13 in the Galactic open cluster M67, which has a turn-off mass of $\sim 1.2\ M_{\odot}$ (see § 2).

The relatively sparse observations of field Population II stars are consistent with the scenario in which CBP does not begin until the μ-barrier is erased (Sneden, Pilachowski, & VandenBerg 1986; Pilachowski et al. 1993, 1997), and are also consistent with our "evolving RGB" CBP models. However, as discussed in Boothroyd & Sackmann (1999), Population II stars in globular clusters

exhibit signs of continuous CBP throughout most or all of the RGB evolution, starting well before the hydrogen shell has erased the μ-barrier (possibly even before deepest first dredge-up), and exhibit more processing at a given metallicity than field Population II stars (see, e.g., Carbon et al. 1982; Trefzger et al. 1983; Langer et al. 1986; Suntzeff & Smith 1991; Boothroyd & Sackmann 1999). Since our models made the assumption that no CBP took place until the μ-barrier was erased, they may be expected to underestimate the amount of processing in globular cluster stars.

The "evolving RGB" models make the reasonable assumption that the extra mixing process continues throughout the subsequent RGB evolution; note that if this is the case, then extra mixing and CBP might occur on the AGB as well. The stellar structure on the AGB of a low mass star is similar to the structure near the tip of the RGB, and thus lithium abundances on the AGB might be produced at a level similar to those predicted at the tip of the RGB by the "evolving RGB" model. On the other hand, the "single episode" models assume that extra mixing terminates before the star's luminosity increases much (e.g., due to spin-down resulting from the RGB mass loss). This is also a possible scenario, but little or no CBP would be expected on the AGB in this case (the driving mechanism being exhausted on the RGB). The post-RGB lithium abundance in this case would be expected to be nearly constant, at whatever value was left behind when CBP turned off on the RGB (probably a low lithium abundance, as the mixing would presumably slow down before stopping, and low $\dot{M}_p$ values yield low lithium abundances — see Figs. 8 and 9c).

For stellar masses above $\sim$ 2.3 $M_\odot$, the RGB ends before the hydrogen shell reaches the μ-barrier, and thus no CBP is expected on the RGB; even if some CBP did take place, these stars spend little time on the RGB, and processing should be negligible. On the early AGB, CBP cannot be extensive, as the hydrogen shell largely stops burning; CBP might take place later on the thermally pulsing AGB, when the hydrogen shell burns strongly (albeit interrupted intermittently by the helium shell flashes). For a fuller discussion, see Boothroyd & Sackmann (1999).

In the present work, extra mixing in both Population I and Population II stars are modelled via a conveyor-belt model of deep circulation similar to that of WBS95, as discussed in § 2. Charbonnel (1995, 1996) and Denissenkov & Weiss (1996) have modelled such mixing in Population II stars using a diffusion algorithm. As discussed in WBS95, these two approaches should yield similar results for the CNO isotopes, since the nuclear processing of CNO isotopes should be insensitive to the speed or geometry of mixing. However, as discussed below, the lighter elements are more dependent on the mixing speed, especially ^{7}Li. They are discussed in detail in the following sections.

3.2.1. ^{7}Li

Figure 7 shows the abundances of the light elements (and ^{12}C/^{13}C) as a function of time on the RGB, for one of our "single episode" CBP models (note that ^{12}C/^{13}C reaches the observed value after 1.25×10^7 yr, but most of the activity in the light elements takes place much earlier; computations were terminated after 5×10^7 yr). It is a key diagram, demonstrating that under

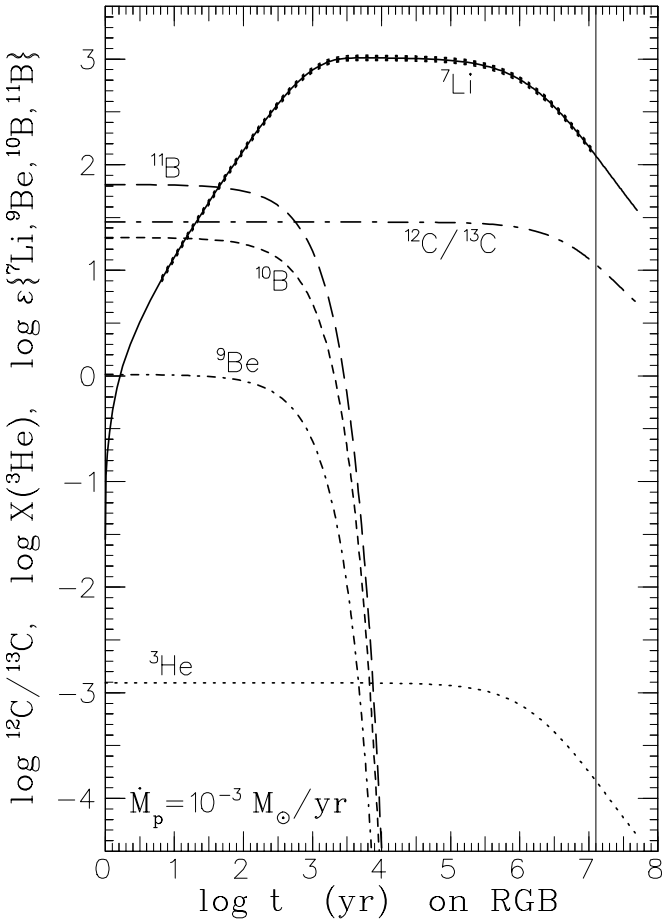

Fig. 7.— The effect of CBP in our "single episode" models, as a function of time on the RGB. These are for a solar metallicity 1 $M_\odot$ star with an envelope mass $M_{\rm env} = 0.7\ M_\odot$ and a mixing rate of deep circulation $\dot{M}_p = 10^{-3}\ M_\odot$/yr; circulation was assumed to reach to $\Delta \log T = 0.17$ from the base of the hydrogen-burning shell, such that the envelope $^{12}C/^{13}C$ ratio reaches the observed value of ~ 11 after a time $t_{\rm mix:RGB} \sim 1.25 \times 10^7$ yr (*vertical line*), although the computations were continued for 5×10^7 yr. The quantities plotted are the log of the $^{12}C/^{13}C$ number ratio, the log of the ^{3}He mass fraction, and log ε values for the other light elements. *Hatched* regions of ^{7}Li curves emphasize cases where abundances are higher than the upper bound of typical RGB field stars.

certain conditions a major amount of ^{7}Li can be created on the RGB due to CBP in a 1 $M_\odot$ star of solar metallicity. Figure 8a shows the ^{7}Li abundances similarly, for various mixing speeds $\dot{M}_p$. One sees that ^{7}Li is enhanced for models with rapid enough circulation (namely, $\dot{M}_p \gtrsim 10^{-4}\ M_\odot$/yr); lower mixing speeds yield lithium destruction.

Figure 9 shows the abundances of the light elements (and $^{12}C/^{13}C$) as a function of luminosity on the RGB, for our "evolving RGB" CBP models with various mixing speeds $\dot{M}_p$. Note that in these models the total mass drops from 0.984 to 0.710 $M_\odot$ (due to mass loss on the RGB), the

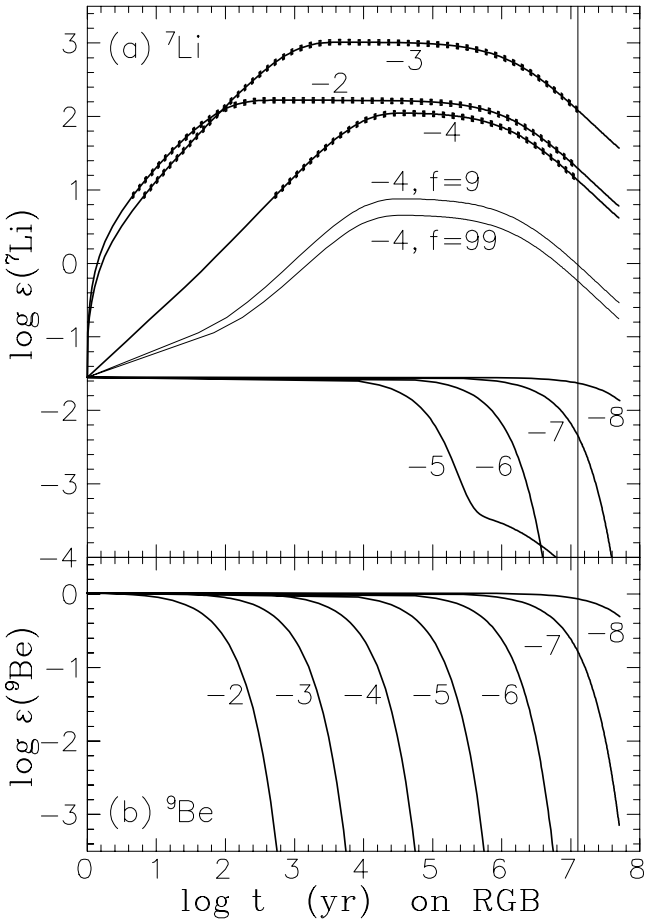

Fig. 8.— (a) Dependence of the ^{7}Li creation and depletion on the mixing speed $\dot{M}_p$ and on our geometry factor $f \equiv f_u/f_d$ in our "single episode" CBP models on the RGB. Curves are labelled by $\log \dot{M}_p$, and by f for cases with $f \neq 1$; hatched regions of curves emphasize high lithium abundance cases (as in Fig. 7). Note that models with $\dot{M}_p < 10^{-7}\ M_\odot$/yr do not produce enough ^{13}C to match the observations by the time $t_{\rm mix:RGB}$ is reached (indicated by *vertical line*). (b) Dependence of ^{9}Be destruction, similarly. Note that boron isotope destruction curves would have the same form, except for having higher initial abundance.

core mass grows from 0.243 to 0.462 $M_\odot$, and the convective envelope mass $M_{\rm env}$ thus drops from 0.718 to 0.246 $M_\odot$ (for lower metallicities or higher stellar masses, these changes are smaller). In these models, the value reached by ^{12}C/^{13}C at the tip of the RGB agrees with the observed values (i.e., the circulation was assumed to operate throughout the RGB); it is essentially independent of the mixing speed or geometry (see Fig. 9a). As in the "single episode" cases, the ^{7}Li abundance is rapidly enhanced for $\dot{M}_p \gtrsim 10^{-4}\ M_\odot$/yr; but even at lower mixing speeds ($\dot{M}_p \gtrsim 10^{-6}\ M_\odot$/yr), significant ^{7}Li enhancements occur as the star climbs the RGB.

The present work shows for the first time that *low mass RGB stars* can also become super-rich

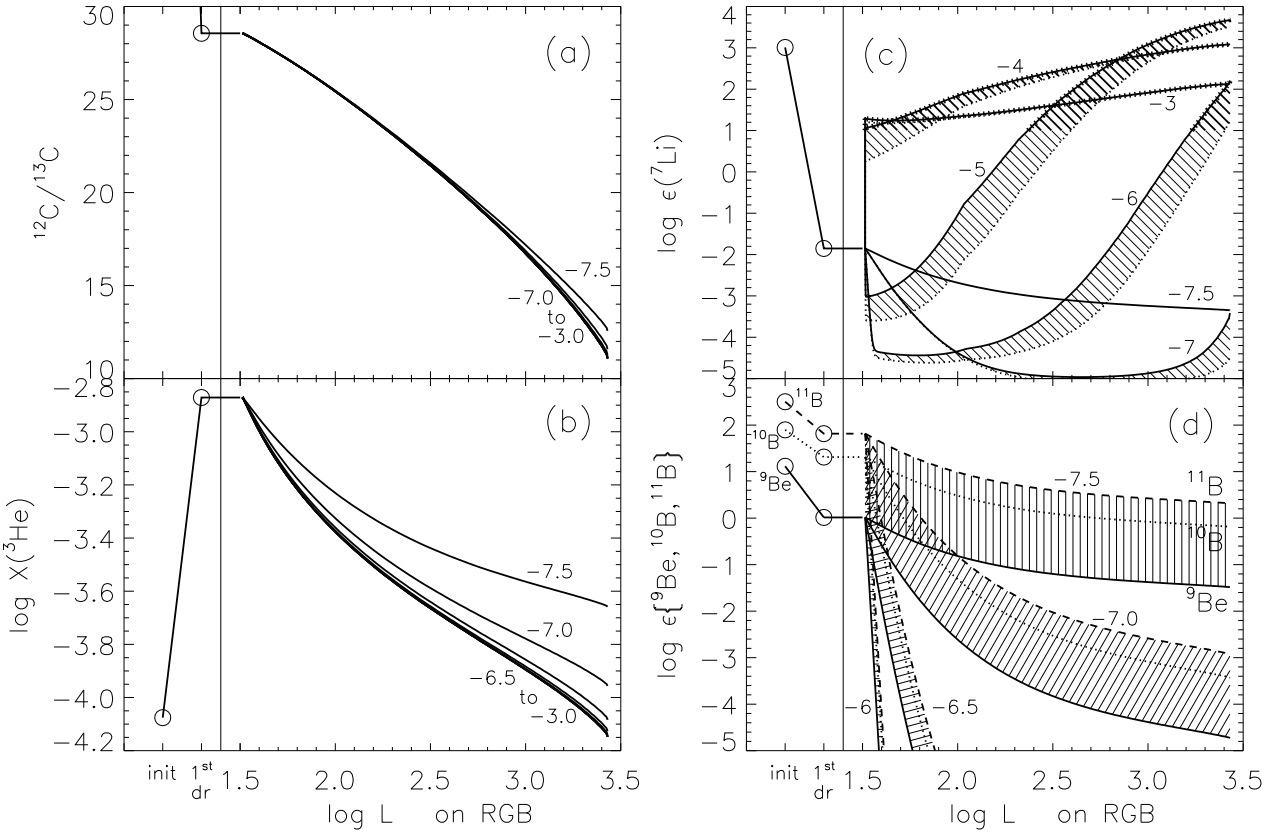

Fig. 9.— The effect of CBP (for various mixing speeds $\dot{M}_p$) in our "evolving RGB" solar metallicity 1 $M_\odot$ CBP models as a function of luminosity on the RGB; curves are labelled by log $\dot{M}_p$. Initial and first dredge-up abundances are shown schematically in the left portion of each panel (open circles). (a) The $^{12}C/^{13}C$ number ratio; the initial ratio (offscale) was 90. (b) The log of the ^3He mass fraction. (c) The log $\varepsilon(^7Li)$ values. The filling between cases with geometry factors $f = 1$ (*solid curves*) and $f = 9$ (*dotted curves*) having the same $\dot{M}_p$ indicates the effect of varying the circulation geometry (see text). Hatched regions of curves and heavy filled regions emphasize high lithium abundance cases, as in Fig. 7. (d) Values of log $\varepsilon(^9Be)$ (*solid curves*), log $\varepsilon(^{10}B)$ (*dotted curves*), and log $\varepsilon(^{11}B)$ (*dashed curves*); low-$\dot{M}_p$ cases are omitted for clarity. Curves for Be and B having the same $\dot{M}_p$ value are connected by filled regions.

lithium stars. This allows one to understand the "K Giant Lithium Problem" (de la Reza & da Silva 1995), of anomalously high lithium abundances discovered in otherwise normal low-mass K giants of relatively low luminosity (Wallerstein & Sneden 1982; Hanni 1984; Brown et al. 1989; Gratton & D'Antona 1989; Pilachowski et al. 1990; Pallavicini et al. 1990; Fekel & Marschall 1991; Fekel & Balachandran 1993; da Silva et al. 1995a, 1995b; de la Reza & da Silva 1995; de la Reza et al. 1996, 1997; Fekel et al. 1996). The presence and amount of lithium creation are critically dependent on the assumed speed $\dot{M}_p$ of extra mixing, as well as on the geometry of mixing (as measured by our factor $f \equiv f_u/f_d$, the fractional area of upward streams relative to downward streams in our

conveyor-belt circulation model). Deeper extra mixing yields higher lithium enhancements for a given (rapid) mixing rate (as may be seen by comparing peak ^{7}Li values from Fig. 8 with the values attained in Fig. 9c near log $L = 1.5$). However, it is noteworthy that the amount of ^{7}Li created does not depend on the previous lithium abundance, i.e., on the lithium history of the star. A qualitative understanding of this mechanism for RGB lithium enrichment is relatively straightforward.

In order to produce the observed additional ^{13}C, the extra mixing must reach temperatures high enough that ^{3}He is also burned (as shown in Figs. 7 and 9), resulting in ^{7}Be creation via $^3\mathrm{He}(\alpha,\gamma)^7\mathrm{Be}$. If the extra mixing is slow, this ^{7}Be is destroyed while still at high temperatures via $^7\mathrm{Be}(p,\gamma)^8\mathrm{B}(e^+\nu)^8\mathrm{Be} \rightarrow 2\alpha$ or $^7\mathrm{Be}(e^-,\nu)^7\mathrm{Li}$, and any ^{7}Li produced from ^{7}Be electron capture is immediately burned up via $^7\mathrm{Li}(p,\alpha)^4\mathrm{He}$. However, for sufficiently high mixing speeds, ^{7}Be can be transported out to cooler regions before the electron capture takes place, where the resulting ^{7}Li can survive and enrich the stellar envelope. In other words, *under special conditions the Cameron-Fowler mechanism can work in low-mass, low-luminosity RGB stars.* The resulting envelope ^{7}Li abundance is determined by the balance between ^{7}Be being transported out (to form ^{7}Li), and ^{7}Li being transported back inwards (and being destroyed). The envelope ^{7}Li abundance reaches equilibrium relative to the abundance of ^{3}He on a timescale $t_{proc} \sim M_{\rm env}/\dot{M}_p$, the time required for circulation to process the entire envelope; t_{proc} is the timescale on which the ^{7}Li abundance reaches its peak values in Figures 7, 8a, and 9c.

The effect on the envelope ^{7}Li abundance of changing the mixing speed $\dot{M}_p$ or the relative areas of upward and downward streams $f \equiv f_u/f_d$ can be readily understood. For mixing speeds $\dot{M}_p > 10^{-7}\ M_\odot$/yr, only a small fraction of the ^{3}He in a circulating blob of matter is destroyed during a single circulation pass, and the total ^{3}He burning rate per unit time is then independent of $\dot{M}_p$ (see Fig. 9b): the amount burned per circulation pass is then inversely proportional to $\dot{M}_p$, and the number of circulation passes per unit time is proportional to $\dot{M}_p$. The amount of ^{7}Be produced per unit time is thus independent of $\dot{M}_p$, but the amount that survives to reach cool temperatures is not. If one increases $\dot{M}_p$, at first the amount of surviving ^{7}Be increases, as does the resulting ^{7}Li production. However, as $\dot{M}_p$ increases still more, there comes a point where essentially all the ^{7}Be survives; the ^{7}Li production rate cannot increase further. The ^{7}Li destruction rate, however, still increases with increasing $\dot{M}_p$ (since all ^{7}Li transported down is burned), and the resulting envelope ^{7}Li abundance decreases with increasing $\dot{M}_p$. The value of $\dot{M}_p^m$ which yields the maximum ^{7}Li production depends on the temperature at the base of the circulation (as may be seen from Fig. 9c, where this temperature grows as the star ascends the RGB). If the circulation speed is less than $\dot{M}_p^m$, then changing the stream geometry will affect the ^{7}Li abundance. Increasing f_u/f_d yields a wider and slower upward stream; less of the ^{7}Be produced at the base of the circulation survives out to cool regions, yielding a lower ^{7}Li abundance (see Fig. 9c).

Figures 7 and 9 show that the peak ^{7}Li abundance can be attained prior to any significant ^{13}C enrichment, but that the ^{7}Li abundance can remain high or even grow during the ^{13}C enrichment process. These preliminary models would thus predict that low mass super-rich lithium stars could occur with $^{12}\mathrm{C}/^{13}\mathrm{C}$ ratios throughout the range from ~ 30 to ~ 4. This is in reasonable agreement

with the observations presented by da Silva et al. (1995a, 1995b), and with the statement of de la Reza et al. (1996) that "the richest Li stars show the smallest $^{12}C/^{13}C$ ratios". The fact that lithium-rich low-mass RGB stars are observed to be rare implies either that few stars attain rapid enough circulation speeds for RGB lithium production, or that rapid circulation speeds are attained only briefly. Recent observations suggest that enhanced RGB lithium abundances occur in conjunction with episodic mass loss in low mass stars, for periods lasting $\sim 10^5$ yr (R. de la Reza 1995, private communication; de la Reza et al. 1996, 1997; Fekel et al. 1996; see also Wallerstein & Morell 1994). This suggests that the extra mixing may be episodic in nature, rather than continuous, providing an additional complication. Short episodes of mixing to a depth rather deeper than assumed in our models could yield $^{12}C/^{13}C$ ratios in agreement with the observations, ^{3}He depletion to an extent comparable to that in our models, and ^{7}Li abundances that could be even larger than in our models (depending on the speed and depth of mixing). Most of the ^{7}Li produced this way would be subsequently destroyed, as the mixing episode died away. An alternative explanation of the above observations invokes variations in the speed (and possibly the depth) of extra mixing, without requiring that it die away completely.

The amount of ^{7}Li injected into the interstellar medium by the observed lithium-rich K giants depends strongly on the parameters of the lithium enrichment scenario, namely, the size and timescales of the lithium enhancements, the magnitude and timescales of the mass loss, and whether, how often, and at what points on the RGB such enhancement episodes recur. For typical parameters from the scenario of de la Reza et al. (1996, 1997), [namely, $\log \varepsilon(^7\mathrm{Li}) \lesssim 4$ for timescales $\lesssim 10^5$ yr, mass loss of $\sim 10^{-7}\ M_\odot$/yr for timescales of ~ 200 yr and $\lesssim 10^{-10}\ M_\odot$/yr thereafter, and recurrence of ~ 10 times per star at $\log L \sim 2$], the *average* ^{7}Li abundance of the total amount of material ejected from low mass stars would be less than 1% of the cosmic abundance — a negligible amount. However, if at least some ^{7}Li enrichment episodes occurred near the tip of the RGB, this average ^{7}Li abundance could be more than an order of magnitude larger, due to the high mass loss rates ($\sim 10^{-7}\ M_\odot$/yr) maintained at the RGB tip for the entire remaining RGB time ($\sim 10^5$ – 10^6 yr), and could yield non-negligible ^{7}Li enrichment of the interstellar medium. In other words, ^{7}Li production via CBP could possibly have a significant impact on the interstellar medium; further observations are needed to pin down the RGB ^{7}Li enhancements simultaneously with the mass loss.

Note that Population II stars are expected to experience more vigorous CBP than Population I stars, with the extra mixing reaching higher temperatures (Boothroyd & Sackmann 1999). Figure 10 shows that low-mass Population II red giants can also become super-rich lithium stars. For high mixing rates ($\dot{M}_p \gtrsim 10^{-4}\ M_\odot$/yr), $\log \varepsilon(^7\mathrm{Li}) \sim 4$ can be attained, a considerably higher abundance than the star was endowed with at birth [$\log \varepsilon(^7\mathrm{Li}) \sim 2$–$3$] and three orders of magnitude higher than the value $\log \varepsilon(^7\mathrm{Li}) \sim 1$ observed in typical Population II subgiants (Pilachowski et al. 1993). Such extremely high lithium abundances can exist only at the onset of CBP, since the ^{3}He fuel for lithium creation is rapidly depleted; however, lithium abundances high enough to be detectable can exist all the way up the RGB (see Fig. 10). For intermediate mixing rates ($\dot{M}_p \sim 10^{-5}\ M_\odot$/yr), lithium is destroyed at the onset of CBP, but near the tip of the RGB enough may be created to

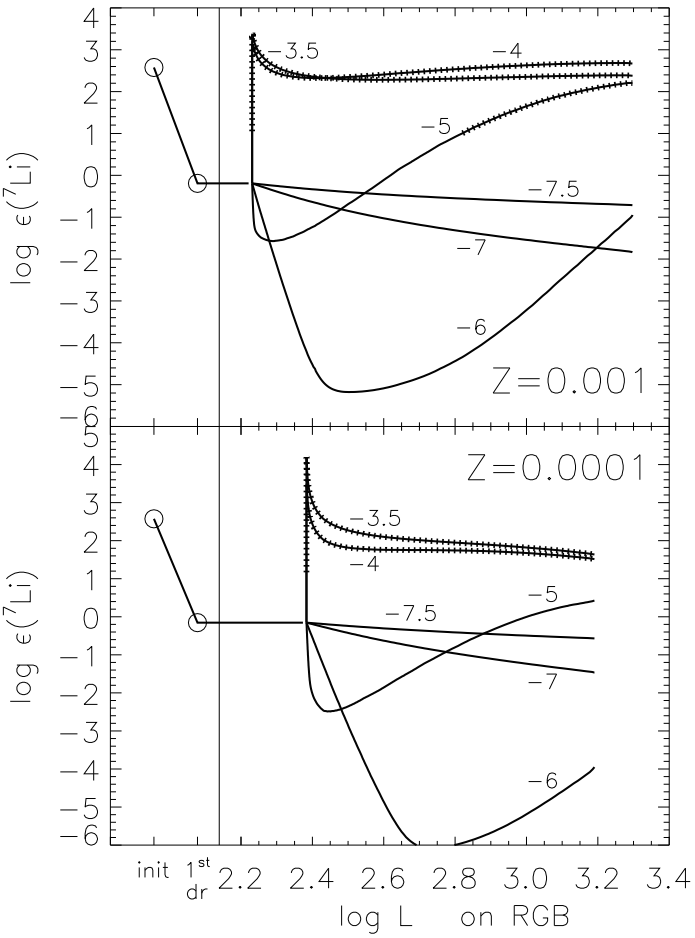

Fig. 10.— The effect of CBP on ^{7}Li in our "evolving RGB" Population II models of 1 $M_\odot$; curves are labelled by the mixing speed, log $\dot{M}_p$. Initial and first dredge-up abundances are shown schematically at left, as in Fig. 9; hatched regions of curves emphasize high lithium abundance cases, as in Fig. 7.

be detectable. For low mixing rates ($\dot{M}_p \sim 10^{-6}\ M_\odot$/yr), lithium is simply destroyed; for very low mixing rates ($\dot{M}_p \sim 10^{-7}\ M_\odot$/yr), lithium destruction is slow enough that lithium may remain detectable for much or even all of the RGB. The effect of varying the geometry factor f was not calculated explicitly in these models, but would be similar to the effect shown (for solar metallicity) in Figure 9c. The trends of Figure 10, relative to Figure 9c, would be exaggerated in any stars where extra mixing reached higher temperatures than assumed in our models; there is observational evidence that this is the case in some Population II stars in globular clusters, as discussed above (see also Boothroyd & Sackmann 1999).

Note that the observations of field Population II subgiants and giants by Pilachowski et al. (1993) find additional lithium depletion on the RGB subsequent to first dredge-up, at the effective temperature where the "μ-barrier" has been erased and CBP is expected to start (Charbonnel 1994,

1995, 1996; Charbonnel et al. 1998; Boothroyd & Sackmann 1999). The lithium depletion in these stars was reproduced by interesting deep mixing models (which we therefore infer to have had low mixing speeds) by Charbonnel (1995, 1996); they can also be reproduced by those Population II "evolving RGB" models of the present work that have $\dot{M}_p \lesssim 10^{-5}\ M_\odot$/yr. Note that Pilachowski et al. (1993) observed 15 Population II RGB stars showing extra lithium depletion (beyond that from first dredge-up), but no stars showing lithium enhancement. It appears that lithium enhancement in field Population II red giants is a rare phenomenon.

If CBP also occurred on the AGB (BSW95; WBS95; Boothroyd & Sackmann 1999), any remaining ^{3}He might then be converted into ^{7}Li, resulting in lithium-rich low-mass AGB stars. Low mass extreme Population II stars, which destroy all their ^{3}He on the RGB (see $Z = 0.0001$ case in Fig. 4), would never be expected ever to become lithium-rich on the AGB.

3.2.2. ^{9}Be, ^{10}B, *and* ^{11}B

Unlike ^{7}Li, the isotopes ^{9}Be, ^{10}B, and ^{11}B cannot be created by CBP; they can only be destroyed. For mixing rates rapid enough that the entire envelope can be processed on the RGB (i.e., $t_{proc} \sim M_{\rm env}/\dot{M}_p \ll \tau_{\rm RGB}$, or $\dot{M}_p \gtrsim 10^{-7}\ M_\odot$/yr), these isotopes are completely destroyed (see Figs. 7, 8b, and 9d); they can be partially preserved only if the mixing is slow enough that only part of the envelope is processed. As may be seen in Figures 7 and 9, the boron isotopes behave very much like ^{9}Be. Figure 8 shows that there exists only a very brief interval when high lithium abundances co-exist with non-zero beryllium (and boron) abundances, as one would expect, since the former is created on the same timescale t_{proc} that the latter are destroyed. Thus low mass lithium-rich RGB stars should almost without exception be completely depleted in beryllium and boron, provided that CBP operates continuously as assumed by our models. If the CBP consists of relatively short-lived episodes (possibly repeated), with each mixing episode reaching higher temperatures than required by a continuous mixing model, then the observed ^{13}C enhancements in Population I stars could be produced in conjunction with enhanced lithium abundances, but large depletions of beryllium and boron need not occur (as only part of the envelope need be mixed down in each episode, due to the short timescale). Thus if one observes enhanced lithium combined with non-zero beryllium and boron, this is probably a signature of episodic deep mixing. So far, no beryllium or boron observations have been made for stars in this CBP stage on the RGB.

3.2.3. ^{3}He

Figures 7 and 9 show that, provided the CBP is strong enough to create the observed enhancement of ^{13}C in a 1 $M_\odot$ star of solar metallicity, there must be an accompanying partial destruction of ^{3}He. This ^{3}He destruction is by a factor of order 10 at the appropriate time ($t \approx 1.25 \times 10^7$ yr) in our "single episode" CBP models, and by a factor of order 20 in our

"evolving RGB" CBP models, for most of the possible range of the speed of extra mixing (namely, $\dot{M}_p \gtrsim 10^{-7}\ M_\odot$/yr). Note that $^{12}C/^{13}C$ observations as a function of RGB luminosity in low mass stars suggest a scenario somewhere between these two models, as discussed in Boothroyd & Sackmann (1999). Since first dredge-up causes a ^{3}He enrichment by a factor of ~ 15 in a $1\ M_\odot$ star (see Fig. 4), CBP results in a reduction of the ^{3}He abundance to roughly its initial value. There is less depletion at higher stellar masses, but more depletion at lower metallicities, as shown in Figure 4. At a minimum, the observed ^{13}C enhancements in solar metallicity stars imply significant ^{3}He depletion; low-metallicity stars, with their large observed carbon depletions on the RGB, must also be almost completely depleted in ^{3}He. Thus low-metallicity stars must be net destroyers of ^{3}He when the contributions of all stellar masses are included, rather than net producers, as standard first dredge-up theory would predict. Solar metallicity stars may be net destroyers of ^{3}He, and surely do not produce very much (again, in contrast to the predictions of standard first dredge-up theory). Note that destruction of ^{3}He has also been obtained by Charbonnel (1995, 1996) in models of extra mixing in low mass metal-poor stars.

One can make more quantitative predictions. First, consider the predictions of standard first and second dredge-up from Figure 4; note also that hot bottom burning yields almost complete ^{3}He destruction in intermediate mass stars ($4 - 7\ M_\odot$ for Population I stars, and $3.5 - 6\ M_\odot$ for Population II stars [Boothroyd & Sackmann 1992]). Weaver & Woosley (1993) estimate that supernovae (from stars with mass $\sim 12 - 40\ M_\odot$) eject material that is depleted in ^{3}He by a factor between 2 and 4. Weighting by the fraction of each star's mass that is ejected and by a Salpeter (1955) initial mass function (IMF) with a typical exponent of $s \approx 2.3 \pm 0.2$, implies that standard first and second dredge-up would result in overall ^{3}He enhancement by a factor $g_3^{\rm dr} \sim 2.4 \pm 0.5$ in Population I stars with masses between 1 and $40\ M_\odot$. If one considers as well the ^{3}He destruction from our "evolving RGB" CBP models, one obtains an overall stellar ^{3}He survival fraction $g_3 \approx 0.8 - 0.9$ (depending on the depletion in supernovae), while our "single episode" CBP models would yield $g_3 \approx 1.0 - 1.1$; an uncertainty of ± 0.2 in the Salpeter IMF exponent s yields an additional uncertainty of only ± 0.1 in g_3. Population II stars, with stronger CBP, would have lower ^{3}He survival fractions: $g_3 \sim 0.6$ for $Z = 0.001$, and $g_3 \sim 0.35$ for $Z = 0.0001$.

A star of $1\ M_\odot$ loses a large fraction of its envelope mass while still on the RGB. Stars of higher mass, however, retain most of their mass until the AGB; thus one may consider the possibility that CBP occurs on the AGB as well as the RGB. Including CBP on the AGB in solar metallicity stars with the same parameters as the "evolving RGB" models yields $g_3 \approx 0.7 - 0.8$; Population II stars would have $g_3 \sim 0.55$ for $Z = 0.001$, and $g_3 \sim 0.3$ for $Z = 0.0001$. If one assumed instead that CBP on the AGB should reproduce observed ^{18}O depletions in low mass AGB stars (which, however, seems unlikely: see Boothroyd & Sackmann 1999), then AGB cool bottom processing would have to be much stronger, yielding $g_3 \sim 0.3$ for solar metallicity and $g_3 \sim 0.2$ for Population II stars.

Recent measurements of high ^{3}He abundances in a few planetary nebulae ejected from low mass stars (Galli et al. 1997) indicate that not quite all low mass stars can experience CBP and ^{3}He depletion, although the fraction that escape CBP on the RGB is only $\sim 4\%$, based on RGB carbon

isotope observations (Charbonnel & do Nascimento 1998). Depending on the exact extent of ^{3}He depletion in RGB stars, Galactic chemical evolution models can accommodate a fairly wide range of primordial deuterium abundances (see, e.g., Olive et al. 1997) — some relaxation is allowed of the lower limit on the cosmic baryon density Ω_b from Big Bang nucleosynthesis calculations. However, Tosi et al. (1998) point out that it is very difficult to contrive a consistent Galactic chemical evolution model that depletes primordial deuterium by more than a factor of 5, let alone the factor of 10 that would be required to accommodate the "high" deuterium observations in quasars.

4. Conclusions

1. It has been demonstrated that ^{7}Li *can be created in low mass red giant stars*, via extra deep mixing and the associated "*cool bottom processing*" (CBP), namely, via the same process which is usually invoked on the red giant branch (RGB) to explain the observed anomalous ^{13}C enhancement, beyond that resulting from first dredge-up. This ^{7}Li production can account for the recent discovery of surprisingly high lithium abundances in some low mass red giants.

2. Lithium is created via the Cameron-Fowler mechanism: ^{7}Be created via ^{3}He$(\alpha,\gamma)^7$Be is transported out fast enough that its electron-capture to ^{7}Li can take place in cool regions, where the resulting ^{7}Li can survive to enrich the stellar envelope. The amount of ^{7}Li produced can exceed $\log \varepsilon(^7\mathrm{Li}) \sim 4$, but depends critically on the details of the extra mixing mechanism (mixing speeds, geometry, episodicity), although it is *independent* of the previous ^{7}Li history of the star.

3. If the deep circulation is a long-lived, continuous process, lithium-rich RGB stars should be completely devoid of beryllium and boron. If it occurs in short-lived episodes, higher ^{7}Li abundances might result, and beryllium and boron might be only partially destroyed.

4. Under some circumstances, CBP in low mass stars can produce *super-rich* lithium stars (i.e., ^{7}Li abundances larger than the interstellar medium value). Low mass stars might possibly be a significant source of ^{7}Li for the interstellar medium.

5. CBP leads to ^{3}He destruction in low mass stars; in contrast to the ^{7}Li creation, the net ^{3}He depletion is largely independent of the details of the extra mixing mechanism. The overall contribution of solar-metallicity stars from 1 to 40 $M_\odot$ is expected to be net destruction of ^{3}He, with an overall ^{3}He survival fraction $g_3 \approx 0.9 \pm 0.2$ (weighted average over all stellar masses); this is in contrast to standard dredge-up theory, which would predict that stars are net producers of ^{3}He (with $g_3^{\mathrm{dr}} \sim 2.4 \pm 0.5$). However, high measured ^{3}He abundances in a few planetary nebulae (Galli et al. 1997) suggest that CBP and ^{3}He depletion do not take place in quite all low mass stars ($\sim 4\%$ escape, according to RGB carbon isotope observations [see Charbonnel & do Nascimento 1998]).

6. Population II stars should experience even more severe ^{3}He depletion than Population I stars ($0.3 \lesssim g_3 \lesssim 0.7$), since they encounter more vigorous processing due to their higher

hydrogen-burning temperatures.

7. This net ^{3}He destruction in stars would result in some relaxation of the upper bound on the primordial (D+^{3}He)/H abundance, but not by much (see, e.g., Olive et al. 1997; Tosi et al. 1998) — high deuterium observations in quasars are still hard to accommodate, and only a slight relaxation is allowed on the lower bound on the cosmic baryon density Ω_b obtained from Big Bang nucleosynthesis calculations.

8. For reference, we also present the effects of standard first and second dredge-up on the helium, lithium, beryllium, and boron isotopes. The first dredge-up dilutions of ^{7}Li, ^{9}Be, ^{10}B, and ^{11}B are typically by factors of $\sim$ 60, 30, 10, and 10, respectively; there is some evidence that extra mixing on the main sequence may result in larger dilution factors. There is also substantial destruction of ^{7}Li by burning during first dredge-up for solar-metallicity stars of $\lesssim 1\,M_\odot$, and during second dredge-up for stars of $\sim 6-7\,M_\odot$.

9. We find that stars of $1-12\,M_\odot$ account for $\sim 50\%$ of the post-Big-Bang interstellar medium enrichment of ^{4}He, with supernovae accounting for the other 50%.

We both are indebted to Charles A. Barnes for support and encouragement as well as insightful discussions, and Robert D. McKeown for the support supplied by the Kellogg Radiation Laboratory. We wish to express a special gratitude to Charles W. Peck and Helmut A. Abt for helpful discussions and support. We are also grateful to G. J. Wasserburg for stimulating discussions and support. One of us (I.-J. S.) wishes to thank Robert F. Christy, her husband, for thoughtful comments and gentlemanly help during the many tasks of daily life. One of us (A. I. B.) wishes to thank Scott D. Tremaine and Peter G. Martin for the support provided by the Canadian Institute for Theoretical Astrophysics. This work was supported in part by a grant from the Natural Sciences and Engineering Research Council of Canada, by a grant from the National Science Foundation PHY 94-20470, by NASA grant NAGW-3337 to G. J. Wasserburg, and by a grant from the Australian Research Council.

REFERENCES

Alexander, D. R., & Ferguson, J. W. 1994, ApJ, 437, 879

Baglin, A., Morel, P. J., & Schatzman, E. 1985, A&A, 149, 309

Balachandran, S. 1991, in Evolution of Stars: The Photospheric Abundance Connection (IAU Symposium 145), ed. G. Michaud & A. Tutukov (Dordrecht: Kluwer), 357

Bania, T. M., Balser, D. S., Rood, R. T., Wilson, T. L., & Wilson, T. J., 1997, ApJS, 113, 353

Blackmon, J. C., Champagne, A. E., Hofstee, M. A., Smith, M. S., Downing, R. G., & Lamaze, G. P. 1995, Phys. Rev. Lett., 74, 2642

Blöcker, T., & Schönberner, D. 1991, A&A, 244, L43

Boesgaard, A. M., & Budge, K. G. 1989, ApJ, 338, 875

Boesgaard, A. M., Heacox, W. D., & Conti, P. S. 1977, ApJ, 214, 124

Boesgaard, A. M., & Tripicco, M. T. 1987, ApJ, 313, 389

Boothroyd, A. I., & Sackmann, I.-J. 1988, ApJ, 328, 653

—. 1992, ApJ, 393, L21

—. 1999, ApJ, 510, in press; preprint astro-ph/9512121

Boothroyd, A. I., Sackmann, I.-J., & Ahern, S. C. 1993, ApJ, 416, 762

Boothroyd, A. I., Sackmann, I.-J., & Fowler, W. A. 1991, ApJ, 377, 318

Boothroyd, A. I., Sackmann, I.-J., & Wasserburg, G. J. 1995, ApJ, 442, L21 (BSW95)

Brown, J. A., Sneden, C., Lambert, D. L., & Dutchover, E., Jr. 1989, ApJS, 71, 293

Cameron, A. G. W. 1955, ApJ, 212, 144

Cameron, A. G. W., & Fowler, W. A. 1971, ApJ, 164, 111

Carbon, D. F., Langer, G. E., Butler, D., Kraft, R. P., Suntzeff, N. B., Kemper, E., Trefzger, C. F., & Romanishin, W. 1982, ApJS, 49, 207

Carlsson, M., Rutten, R. J., Bruls, J. H. M. J., & Shchukina, N. G. 1994, A&A, 288, 860

Carswell, R. F., Rauch, M., Weymann, R. J., Cooke, A. J., & Webb, J. K. 1994, MNRAS, 268, L1

Caughlan, G. R., & Fowler, W. A. 1988, Atomic Data Nucl. Data Tables, 40, 205

Chaboyer, B., Demarque, P., & Pinsonneault, M. H. 1995, ApJ, 441, 876

Charbonnel, C. 1994, A&A, 282, 811

—. 1995, ApJ, 453, L41

—. 1996, in Proc. of "From Stars to Galaxies", Crete 9-13 Oct. 1995, ASP Conf. Ser. Vol. 98, ed. C. Leitherer, U. Fritz-von Alvensleben, & L. Hucra (ASP: San Francisco), 213

Charbonnel, C., Brown, J. A., & Wallerstein, G. 1998, A&A, 332, 204

Charbonnel, C., & do Nascimento, J. D., Jr. 1998, A&A, 336, 915

Charbonnel, C., Vauclair, S., & Zahn, J.-P. 1992, A&A, 255, 191

D'Antona, F. & Mazzitelli, I. 1984, A&A, 138, 431

da Silva, L., de la Reza, R., & Barbuy, B. 1995a, in Stellar and Interstellar Lithium and Primordial Nucleosynthesis: IAU Joint Discussion 11, Memorie della Società Astronomica Italiana, Vol. 66, No. 2, ed. F. Spite & R. Pallavicini (Firenza: Soc. Astron. Italiana), 417

—. 1995b, ApJ, 448, L41

Dearborn, D. S. P. 1992, Phys. Reports, 210, 367

Dearborn, D., Eggleton, P. P., & Schramm, D. N. 1976, ApJ, 203, 455

Dearborn, D. S. P., Steigman, G., & Tosi, M. 1996, ApJ, 465, 887; 1996, ApJ, 473, 570

de la Reza, R., & da Silva, L. 1995, ApJ, 439, 917

de la Reza, R., Drake, N. A., & da Silva, L. 1996, ApJ, 456, L115

de la Reza, R., Drake, N. A., da Silva, L., & Torres, C. A. O. 1997, ApJ, 482, L77

Deliyannis, C. P., Boesgaard, A. M., & King, J. R. 1995, ApJ, 452, L13

Denissenkov, P. A., & Weiss, A. 1996, A&A, 308, 773

Duncan, D. K., Peterson, R. C., Thorburn, J. A., & Pinsonneault, M. H. 1994, BAAS, 26, 868

—. 1998, ApJ, in press

Fekel, F. C., & Balachandran, S. 1993, ApJ, 403, 708

Fekel, F. C., & Marschall, L. A. 1991, AJ, 102, 1439

Fekel, F. C., Webb, R. A., White, R. J., & Zuckerman, B. 1996, ApJ, 462, L95

Galli, D., Palla, F., Ferrini, F., & Penco, U. 1995, ApJ, 443, 536

Galli, D., Stanghellini, L., Tosi, M., & Palla, F. 1997, ApJ, 477, 218

Galli, D., Palla, F., Straniero, O., & Ferrini, F. 1994, ApJ, 432, L101

Genova, F., & Schatzman, E. 1979, A&A, 78, 323

Gilroy, K. K. 1989, ApJ, 347, 835

Gilroy, K. K., & Brown, J. A. 1991, ApJ, 371, 578

Gratton, R. G., & D'Antona, F. 1989, A&A, 215, 66

Grevesse, N. 1984, Phys. Scripta, T8, 49

Guzik, J. A., & Cox, A. N. 1995, ApJ, 448, 905

Hanni, L. 1984, Sov. Astron. Lett., 10, 51

Hobbs, L. M., & Pilachowski, C. 1988, ApJ, 334, 734

Hogan, C. J. 1995, ApJ, 441, L17

Iben, I., Jr. 1967, ApJ, 147, 624

—. 1975, ApJ, 196, 525

Iglesias, C. A., & Rogers, F. J. 1996, ApJ, 464, 943

Lambert, D. L., Dominy, J. F., & Sivertsen, S. 1980, ApJ, 235, 114

Landré, V., Prantzos, N., Aguer, P., Bogaert, G., Lefebvre, A., & Thibaud, J. P. 1990, A&A, 240, 85

Langer, G. E., Kraft, R. P., Carbon, D. F., & Friel, E. 1986, PASP, 98, 473

Lattanzio, J. C. 1992, Proc. Astr. Soc. Australia, 10, 120

Michaud, G., & Charbonneau, P. 1991, Space Sci. Rev., 57, 1

Olive, K. A., Schramm, D. N., Scully, S. T., & Truran, J. W. 1997, ApJ, 479, 752

Pallavicini, R., Randich, S., Giampapa, M., & Cutispoto, G. 1990, Messenger, 62, 51

Pilachowski, C. A., Sneden, C., & Booth, J. 1993, ApJ, 407, 699

Pilachowski, C. A., Sneden, C., Hinkle, K., & Joyce, R. 1997, AJ, 114, 819

Pilachowski, C. A., Sneden, C., & Hudek, D. 1990, AJ, 99, 1225

Pinsonneault, M. H., Deliyannis, C. P., & Demarque, P. 1992, ApJS, 78, 181

Pinsonneault, M. H., Kawaler, S. D., Sofia, S., & Demarque, P. 1989, ApJ, 338, 424

Proffitt, C. R., & Michaud, G. 1989, ApJ, 346, 976

—. 1991, ApJ, 380, 238

Reimers, D. 1975, in Problems in Stellar Atmospheres and Envelopes, ed. B. Bascheck, W. H. Kegel, & G. Traving (New York: Springer), 229

Rood, R. T., Bania, T. M., Balser, D. S., & Wilson, T. L. 1998, in The Primordial Nuclei and their Galactic Evolution, ed. N. Prantzos, M. Tosi, & R. von Steiger (Kluwer: Dordrecht), 185

Rood, R. T., Bania, T. M., & Wilson, T. L. 1984, ApJ, 280, 629

Rugers, M., & Hogan, C. J. 1996a, ApJ, 459, L1

—. 1996b, AJ, 111, 2135

Rugers, M. H., & Hogan, C. J. 1997, preprint astro-ph/9702058

Sackmann, I.-J., & Boothroyd, A. I. 1992, ApJ, 392, L71

—. 1995, in Stellar and Interstellar Lithium and Primordial Nucleosynthesis: IAU Joint Discussion 11, Memorie della Società Astronomica Italiana, Vol. 66, No. 2, ed. F. Spite & R. Pallavicini (Firenza: Soc. Astron. Italiana), 403

—. 1999, in preparation

Sackmann, I.-J., Boothroyd, A. I., & Fowler, W. A. 1990, ApJ, 360, 727

Sackmann, I.-J., Boothroyd, A. I., & Kraemer, K. E. 1993, ApJ, 418, 457

Sackmann, I.-J., Smith, R. L., & Despain, K. H. 1974, ApJ, 187, 555

Salpeter, E. E. 1955, ApJ, 121, 161

Scalo, J. M., Despain, K. H., & Ulrich, R. K. 1975, ApJ, 196, 805

Schatzman, E. 1977, A&A, 56, 211

Sharp, C. M. 1992, A&AS, 94, 1

Smith, G. H., & Tout, C. A. 1992, MNRAS, 256, 449

Smith, V. V., & Lambert, D. L. 1989, ApJ, 345, L75

—. 1990, ApJ, 361, L69

Sneden, C., Pilachowski, C. A, & VandenBerg, D. A. 1986, ApJ, 311, 826

Songaila, A., Cowie, L. L., Hogan, C. J., & Rugers, M. 1994, Nature, 368, 599

Steigman, G. 1985, in Nucleosynthesis: Challenges and New Developments, ed. W. D. Arnett & J. W. Truran (U. of Chicago Press: Chicago), 48

Steigman, G., & Tosi, M. 1992, ApJ, 401, 150

Suntzeff, N. B., & Smith, V. V. 1991, ApJ, 381, 160

Sweigart, A. V., & Mengel, J. G. 1979, ApJ, 229, 624

Swenson, F. J., & Faulkner, J. 1992, ApJ, 395, 654

Timmes, F. X., Woosley, S. E., & Weaver, T. A. 1995, ApJS, 98, 617

Tosi, M., Steigman, G., Matteucci, F., & Chiappini, C. 1998, ApJ, 498, 226

Trefzger, C. F., Carbon, D. F., Langer, G. E., Suntzeff, N. B., & Kraft, R. P. 1983, ApJ, 266, 144

Tytler, D., & Fan, X., 1994, BAAS, 26, 1424

Tytler, D., Fan, X. M., & Burles, S. 1996, Nature, 381, 207

Tytler, D., Burles S., & Kirkman, D. 1996, preprint astro-ph/9612121

VandenBerg, D. A., & Poll, H. E. 1989, AJ, 98, 1451

Vangioni-Flam, E., Olive, K. A., & Prantzos, N. 1994, ApJ, 427, 618

Vauclair, S. 1988, ApJ, 335, 971

Vauclair, S., & Charbonnel, C. 1995, A&A, 295, 715

Walker, T. P., Steigman, G., Schramm, G., Olive, K. A., & Kang, H.-S. 1991, ApJ, 376, 51

Wallerstein, G., & Morell, O. 1994, A&A, 281, L37

Wallerstein, G., & Sneden, C. 1982, ApJ, 255, 577

Wasserburg, G. J., Boothroyd, A. I., & Sackmann, I.-J. 1995, ApJ, 447, L37 (WBS95)

Weaver, T. A., & Woosley, S. E. 1993, Phys. Rept., 227, 65

Webb, J. K., Carswell, R. F., Lanzetta, K. M., Ferlet, R., Lemoine, M., Vidal-Madjar, A., & Bowen, D. V. 1997, Nature, 388, 250

Weidemann, V. 1984, A&A, 134, L1

Weidemann, V., & Koester, D. 1983, A&A, 121, 77

Weiss, A., Wagenhuber, J., & Denissenkov, P. A. 1996, A&A, 313, 581

Whitmire, D. P., Doyle, L. R., Reynolds, R. T., & Matese, J. J. 1995, J. Geo. Research Planets, 100, 5457

Yang, J., Turner, M. S., Steigman, G., Schramm, D. N., & Olive, K. A. 1984, ApJ, 281, 493
